ARR No. L5A13

NATIONAL ADVISORY COMMITTEE FOR AERONAUTICS

WARTIME REPORT

ORIGINALLY ISSUED
February 1945 as
Advance Restricted Report L5A13

THE INFLUENCE OF VERTICAL-TAIL DESIGN AND DIRECTION OF PROPELLER ROTATION ON TRIM CHARACTERISTICS OF A TWIN-ENGINE-AIRPLANE MODEL WITH ONE ENGINE INOPERATIVE

By Marvin Pitkin, John W. Draper, and Charles V. Bennett

Langley Memorial Aeronautical Laboratory
Langley Field, Va.

NACA

WASHINGTON

NACA ARR No. L5A13

NATIONAL ADVISORY COMMITTEE FOR AERONAUTICS

ADVANCE RESTRICTED REPORT

THE INFLUENCE OF VERTICAL-TAIL DESIGN AND DIRECTION OF PROPELLER ROTATION ON TRIM CHARACTERISTICS OF A TWIN-ENGINE-AIRPLANE MODEL WITH ONE ENGINE INOPERATIVE

By Marvin Pitkin, John W. Draper, and Charles V. Bennett

SUMMARY

Tests have been made in the Langley free-flight tunnel to determine the influence of mode of propeller rotation and vertical-tail design upon the trim characteristics of a model of a twin-engine airplane with one engine inoperative. The test model was mounted on a trim stand, which allowed freedom in roll and yaw under conditions simulating those required by the NACA and the Army Air Forces for asymmetric-power operation in flight. The seven vertical-tail designs tested included three tails of low aspect ratio and of different area, one twin tail of low aspect ratio, two tails of high aspect ratio and with different rudder areas, and one all-movable tail of high aspect ratio equipped with a linked tab. All tests were made with the flaps down.

The tests showed that the effect of mode of propeller rotation upon the directional trim characteristics of the model operating with asymmetric power was considerable. Propeller rotation in which the upper tips rotate outboard toward the wing tip (outboard rotation) generally created more severe out-of-trim conditions than inboard rotation.

The all-movable tail design was found to be more effective than the other designs tested in nullifying the effects of asymmetric power. The conventional tail designs with high aspect ratio were more effective than the designs with low aspect ratio in this respect. The single vertical tails were generally more effective in trimming the yawing moments created by asymmetric power than twin vertical tails of the same aspect ratio and equal

area, particularly when the rudder was free. At small angles of sideslip, however, the moments caused by asymmetric power were more readily trimmed by deflecting the rudders of the twin tails than by deflecting the rudder of a single tail.

The trimming effectiveness of the vertical tail increased almost directly with vertical-tail area but increased at a decreasing rate with rudder deflection and chord.

When the rudder was free, the addition of dorsal- and ventral-fin areas permitted increases in the asymmetric power balanced by the tail surface at moderate angles of sideslip.

INTRODUCTION

The failure of one or more engines of multiengine airplanes introduces a sudden and severe demand upon the directional stability and control of those airplanes. Such failures result in the instantaneous application of large yawing moments that must be neutralized either by the rudder control or by the directional stability of the airplane. In addition, asymmetric power conditions create rolling moments that must be balanced by aileron deflection in order to maintain straight flight. This aileron deflection creates additional yawing moments that require further trimming by the vertical tail surfaces. For multiengine airplanes, then, the asymmetric power condition generally imposes the most severe requirements for directional stability and control and to a large extent dictates the design of the vertical tail surfaces of these airplanes.

An investigation has therefore been carried out in the Langley free-flight tunnel to provide data concerning the relative merits of seven vertical-tail designs and two modes of propeller rotation under conditions of asymmetric power. The NACA and Army flying-qualities requirements (references 1 and 2) for directional stability and control of airplanes operating with asymmetric power were used to establish the test conditions. The results of the investigation are reported herein.

A $\frac{1}{20}$-scale model of a conventional twin-engine airplane in the medium-bomber class (the North American B-28 airplane) was used in the tests. The model was mounted on a test stand, which allowed freedom in yaw and roll. The effects of asymmetric power could thus be visually observed from changes in the model attitude.

The seven vertical-tail designs studied in this investigation varied in either aspect ratio, total tail area, rudder area, or general arrangement. Tests were made with rudders fixed and free, and the effects of adding various dorsal and ventral fins were studied with the rudders free. The effect of mode of rotation of the operating propeller upon the vertical-tail characteristics was investigated for all tail arrangements. All tests were made with the flaps down.

SYMBOLS

C_L lift coefficient $\left(\frac{\text{Lift}}{qS_w}\right)$

C_l rolling-moment coefficient $\left(\frac{\text{Rolling moment}}{qS_wb_w}\right)$

C_n yawing-moment coefficient $\left(\frac{\text{Yawing moment}}{qS_wb_w}\right)$

C_{n_β} rate of change of yawing-moment coefficient with angle of sideslip $\left(\frac{\partial C_n}{\partial \beta}\right)$

T_c thrust coefficient for one engine $\left(\frac{T_e}{\rho V^2 D^2}\right)$

D propeller diameter, feet

ρ density of air, slug per cubic foot

V free-stream airspeed, feet per second

$V_{\text{take-off}}$ velocity at end of take-off run, feet per second

V_{min} stalling speed with flaps down, feet per second

q free-stream dynamic pressure, pounds per square foot $\left(\frac{1}{2}\rho V^2\right)$

T_e effective thrust of one engine, pounds

η propeller efficiency, percent

W gross weight, pounds

S_w wing area, square feet

bhp brake horsepower of full-scale airplane simulated by model

thp thrust horsepower

δ_a combined aileron deflection, degrees

δ_r rudder deflection, positive when trailing edge is to left, degrees

δ_f flap deflection, positive when trailing edge is down, degrees

δ_e elevator deflection, degrees

δ_T tab deflection of all-movable tail, positive when trailing edge is to left, degrees

i_t tail incidence of all-movable tail with respect to center line of fuselage, degrees

α angle of attack, degrees

α_t local angle of attack of vertical tail, degrees

β angle of sideslip, degrees

A aspect ratio of vertical tail $\left(b_t^2/S_t\right)$

S_t area of vertical tail, square feet

S_b balance area of rudder, percent rudder area

S_r rudder area, square feet

b_t span of vertical tail, feet

b_w wing span, feet

APPARATUS

Wind Tunnel

The tests were made in the Langley free-flight tunnel, a complete description of which will be found in reference 3. The tunnel was locked at an angle of pitch of 0° for all tests.

Trim Stand

All tests were made on a trim stand, which was securely fastened to the floor of the wind tunnel. This stand was so constructed as to allow the model freedom in roll and yaw about the stability axes of the model. The stability axes are a system of axes in which the Z-axis is in the plane of symmetry of the airplane perpendicular to the relative wind. The X-axis is in the plane of symmetry perpendicular to the Z-axis. The Y-axis is perpendicular to the plane of symmetry. The origin of the stability axes is at the center of gravity of the airplane, which for the present tests was located on the fuselage center line 25 percent of the mean aerodynamic chord behind the leading edge.

Photographs of the model mounted on the trim stand are given as figure 1 and the construction of the stand is illustrated in figure 2. Figure 2 shows that bearing A permits freedom in roll and bearing B permits freedom in yaw. A calibrated coil spring was inserted in bearing A to provide stability in roll. This alteration made possible the measurement of unbalanced rolling moments as a function of the angle of bank and thereby facilitated the trimming of these moments by means of aileron deflection. Both bearings A and B were equipped with ball bearings to keep frictional effects to a minimum.

The trimming fin shown in figure 2 was added to the trim stand to neutralize the drag yawing moments caused when the wind was on by the forward struts at an angle of yaw. Since this fin area was such that the trim stand was in complete equilibrium of yawing moments $\left(C_{n_\beta} = 0\right)$ over the yaw range tested, the trim stand did not affect the directional stability characteristics of the model.

Model

The model used in the investigation was a $\frac{1}{20}$-scale model of the North American B-28 airplane. A three-view drawing and a photograph of the model are given as figures 3 and 4, respectively.

The model was equipped with 2 four-blade propellers having a diameter of 8.50 inches and set at an angle of pitch of 20°. Power was furnished by a direct-current controllable-speed electric motor rated 1/8 horsepower at 15,000 rpm. The left propeller, which was kept inoperative during the tests, was so mounted as to windmill freely. The right propeller, which was used as the operating propeller for all tests, was geared to the motor at a ratio of 1:3. Provision was made for reversal of the direction of propeller rotation. The model was equipped with partial-span slotted flaps (fig. 3), which were deflected 45° for all tests.

Sketches of the vertical-tail designs used in the investigation are shown in figure 5 and sketches of the dorsal- and ventral-fin areas utilized in the rudder-free tests, in figure 6. Tail 2 represents the original vertical tail surface of the full-scale airplane and is considered typical of conventional vertical-tail design. The dimensional characteristics of this tail were varied to form the other vertical-tail designs. All vertical tails were constructed of the NACA 0012 section. In order to maintain similitude of hinge-moment characteristics as far as practicable, all rudders were of identical blunt-nose balance type with a balance area 12.2 percent of the rudder area. This type of rudder is of negative floating tendency and trails with the wind when free.

The dimensional characteristics of the full-scale airplane are given in the following table:

Wing:

Area, sq ft	675.90
Span, ft	72.61
Aspect ratio	7.80
Root chord, in.	161.13
Tip chord, in.	67.00
Mean aerodynamic chord, in.	120.09
Root section	NACA 23017

Tip section	NACA 4409R
Percent chord line with zero sweepback	33
Sweepback at leading edge, deg	4.2
Dihedral angle, deg	2
Incidence, deg	3
Geometric twist (washout), deg	2.5
Taper ratio	2.4:1

Fuselage:

Length, ft	54.5
Section	Circular
Frontal area, sq ft	38.5

Horizontal tail:

Total area, sq ft	183.20
Span, ft	26.85
Aspect ratio	3.94
Dihedral angle, deg	0
Stabilizer setting, deg	1.50
Length from hinge of elevator to center of gravity of airplane, ft	28.90
Elevator balance area, sq ft	10.63
Elevator area behind center line of hinge, sq ft	53.30

Vertical tail 2:

Total area, sq ft	74.90
Span, ft	10.68
Aspect ratio	1.54
Length from hinge line of rudder to center of gravity of airplane, ft	27.40
Fin area, sq ft	35.66
Rudder area, sq ft	39.24
Rudder-balance area, sq ft	9.14
Rudder area behind hinge line, sq ft	30.10

(Pertinent data for tails 1, 3, 4, 5, 6, and 7 are given in fig. 5.)

Aileron (one of two):

Area behind hinge line, sq ft	20.91
Span, ft	11.41
Mean chord, in.	17.0

Flap:

Total flap area, sq ft	80.3
Total span, ft	38.4
Type	Slotted

SPECIFICATIONS AND CRITERIONS

The NACA and Army flight requirements for multiengine airplanes operating with asymmetric power were chosen to establish the proper test conditions. No separate attempt was made to reproduce the Navy specifications for asymmetric power because of the close similarity between the Navy and the NACA specifications.

Specifications for Directional Control

(Rudder Fixed)

The NACA and Army specifications (references 1 and 2, respectively) for directional control of airplanes operating with asymmetric power are as follows:

NACA requirement (II-E) 3.- "The rudder control should be sufficiently powerful to provide equilibrium of yawing moments at zero sideslip at all speeds above 110 percent of the minimum take-off speed under the following conditions:

> a. Airplanes with two or three engines:
> With any one engine inoperative (propeller in low pitch) and the other engine or engines developing full rated power."

Army requirement E-2c(1)(c).- "The rudder control shall be powerful enough to trim a multi-engine airplane for straight flight with less than 10 degrees of sideslip at 1.2 V_{s_h} [V_{s_h} = stalling speed of the airplane, throttles closed, gear down, flaps in best take-off condition] when the throttle on an outboard engine is abruptly closed (propeller in low pitch) and the other engine or engines are developing full take-off power. The flaps shall be in the take-off setting, and the gear shall be down...."

Specifications for Directional Stability

(Rudder Free)

The NACA specification (requirement (II-F) 4 of reference 1) relating to the requirements for directional stability with rudder free under asymmetric power conditions is as follows:

"The yawing moment due to sideslip (rudder free with airplane trimmed for straight flight on symmetric power) should be such that straight flight can be maintained by sideslipping at every speed above 140 percent of the minimum speed with rudder free with extreme asymmetry of power possible by the loss of one engine."

Criterion for Vertical-Tail Effectiveness

under Asymmetric Power Conditions

Each of the specifications previously listed requires the directional control or the directional stability of the airplane in question to be sufficiently powerful to balance the yawing moments created by asymmetric power under certain specified flight conditions. It follows that the vertical-tail effectiveness in flight may be gaged by the maximum amount of asymmetric power which such a tail can balance under the specified conditions. In this investigation, therefore, the maximum asymmetric power permissible under the airspeed and trim conditions specified by the Army and the NACA was used to evaluate the effectiveness of the vertical tails tested.

It should be observed that the flight specifications require that straight flight or complete equilibrium of lateral forces and moments be maintained. In order to maintain such equilibrium in flight, the ailerons must be deflected so that the rolling moments caused by asymmetric power are balanced and the airplane assumes an attitude of bank, which nullifies the side force created by rudder deflection and/or angle of sideslip. Inasmuch as an attitude of bank does not affect the trim requirements of the vertical tail surface, no attempt was made in the tests to simulate the balance of side force by angle of bank. Aileron deflection, however, directly affects directional trim by virtue of the yawing moments created by such deflections. Consequently, the ailerons were so adjusted

for all tests as to maintain complete balance of aerodynamic rolling moments and thereby to simulate flight conditions correctly.

TESTS

Test Conditions

The test lift coefficient was established from consideration of the specified airspeeds in the Army and NACA requirements. These values were converted to lift-coefficient forms as follows:

The NACA requirement (II-E) 3 a (rudder fixed) specifies an airspeed equal to 1.10 times the take-off speed. If $V_{take\text{-}off}$ is assumed equal to $1.2V_{min}$, the airspeed requirement for this specification is equal to $1.32V_{min}$. If the maximum lift coefficient of the B-28 airplane is assumed equal to 2.0, the specified lift coefficient corresponding to $1.32V_{min}$ is defined by the expression $2.0\left(\frac{V_{min}}{1.32V_{min}}\right)^2$ which equals 1.15. In a similar manner, the lift coefficient necessary to satisfy NACA requirement (II-F) 4 (rudder free) was found to be 1.02. The lift coefficient necessary to satisfy the Army requirement (rudder fixed) was calculated as 1.39. Because it was assumed that slight changes in lift coefficient would not affect the model test results if the correct values of thrust coefficient were used, all tests were run at a constant angle of attack of 5°, which corresponded to a lift coefficient of 1.10.

All tests were run at a test velocity of 40 feet per second, which corresponds to a test Reynolds number of 128,000 based on the mean aerodynamic chord of 0.503 foot. The aileron deflections for all tests were adjusted to provide equilibrium of rolling moments.

Test Procedures

Rudder fixed.- In the tests with rudder fixed, the model was mounted on the stand with the rudder deflected in the direction that counteracted the yaw caused by

asymmetric power. Measurements were then taken of the maximum amount of asymmetric thrust the rudder would balance at angles of yaw of 0° and 10° for rudder deflections of 0°, 5°, 10°, 20°, and 30°.

Rudder free.- The tests with rudder free were made by measuring the amount of asymmetric thrust and angle of yaw produced by asymmetric power for various angles of yaw up to the angle at which directional instability was encountered. Tests with rudder free were made of the model with each of the following vertical-tail arrangements:

(1) Vertical tail alone

(2) Vertical tail plus dorsal fin a

(3) Vertical tail plus dorsal fin b

(4) Vertical tail plus ventral fin a

(5) Vertical tail plus ventral fin a plus dorsal fin a

The absolute dorsal- and ventral-fin areas required for each test were determined from the percentages of the vertical tails being tested given in figure 6. No tests were made to determine the influence of auxiliary fin area upon the characteristics of twin tail 4.

Power calculations.- The thrust coefficients that were obtained in the tests of the model were converted to the simulated asymmetric brake horsepower of the full-scale airplane by means of the relationship

$$bhp = \frac{thp}{\eta}$$

$$= \frac{T_e V}{550\eta}$$

or

$$bhp = \frac{T_c \left(2\frac{W}{S_w}\right)^{3/2} D^2}{550\eta_o C_L^{1/2}} \qquad (1)$$

The full-scale propeller efficiency η was assumed to be equal to 0.75 for the calculations. Values of wing loading W/S_W and propeller diameter D were obtained from the full-scale characteristics of the North American P-28 airplane and were equal to 47.5 pounds per square foot and 14.7 feet, respectively. The value of the mass density of air ρ was chosen as 0.00238, which is its value at sea level under standard atmospheric conditions. Substitution of these values in equation (1) yields the relationship

$$bhp = \frac{T_c}{C_L^{3/2}} 9900 \tag{2}$$

The values of C_L in equation (2) are those corresponding to the airspeed specified in the Army and the NACA requirements and were determined as shown in the section entitled "Test Conditions." Substituting these values of lift coefficient in equation (2) yields the expressions defining the conversion of model thrust coefficient T_c to the estimated full-scale brake horsepower, which are:
For rudder fixed,

NACA requirement

$$bhp = 8050T_c \tag{3}$$

Army requirement

$$bhp = 8070T_c \tag{4}$$

For rudder free,

NACA requirement

$$bhp = 9620T_c \tag{5}$$

RESULTS AND DISCUSSION

The data obtained in the investigation are plotted in figures 7 to 18. Figure 7 shows the rolling-moment coefficients produced by the ailerons used in the tests. Figures 8 to 10 present the values of the asymmetric-thrust coefficient balanced by means of rudder deflection.

Figures 11 to 13 give the values of the asymmetric-thrust coefficient balanced by the yawed model with rudder free. Data showing the influence of dorsal- and ventral-fin areas upon trim characteristics are presented in figures 14 to 18.

The test data in figures 8 to 13 were rearranged and converted to values of full-scale brake horsepower in figures 19 to 24. An index to all figures is presented as table I.

Effect of Mode of Propeller Rotation

The mode of propeller rotation in which the upper blade tips move toward the fuselage is henceforth designated inboard rotation. The rotation in which the upper blade tips move out toward the wing tip is designated outboard rotation. Almost all conventional airplanes are equipped with right-hand propellers. On multiengine airplanes, the direction of propeller rotation with respect to the wing tips (inboard or outboard) is therefore determined by the location of the propeller. If the right engine fails, the direction of the operating propeller rotation is inboard and the airplane yaws in a positive sense. For left-engine failures, the operating propeller rotates outboard and the airplane yaw is negative. The results of the present investigation show that use of different modes of propeller rotation caused considerable difference in trim characteristics of an airplane operating under asymmetric power.

With only one exception, the data presented in figures 8 to 13 indicate that the use of outboard propeller rotation decreased the values of permissible asymmetric-thrust coefficient balanced by any given vertical-tail configuration and that this mode of rotation would therefore determine the minimum vertical-tail size. The exception occurred when twin tail 4 operated under the Army specifications (fig. 9); in these tests inboard rotation was less favorable than outboard rotation.

The difference in asymmetric power balanced by a given tail arrangement with either of the two modes of rotation appeared to increase in magnitude with the amount of directional stability and of control being applied. The largest differences occurred at large rudder angles and for tails 5, 6, and 7, which have high aspect ratios. Particularly large effects of propeller rotation were observed when the rudder was free.

The magnitude of effect of reversing the propeller rotation has been illustrated in figure 19. This figure presents the calculated values of permissible brake horsepower for both modes of propeller rotation for the representative rudder deflection of 20° (figs. 19(a) and 19(b)) and for that angle of sideslip at which directional instability was encountered in the tests with rudder free (fig. 19(c)). This angle of sideslip was between 10° and 12° for almost all the conditions tested. The results presented in figure 19 show that the difference in asymmetric power balanced by the vertical tail for inboard and outboard rotation was about 400 horsepower for most conditions and was as large as 1000 horsepower for some.

The effects of changing the direction of propeller rotation appear to be explained by the data of reference 4. Reference 4 concludes that use of inboard propeller rotation with the flaps down caused the slipstream to converge toward the tail and thereby increased the contribution of the tail surfaces to directional stability for small to moderately large angles of yaw. This slipstream displacement would result in a beneficial effect of inboard rotation upon the trimming action of the vertical tail surfaces, particularly for twin tail 4, which under NACA specifications ($\beta = 0^{\circ}$) appears to be partly immersed in the slipstream jet. Reference 4 also concludes that outboard rotation causes the slipstream jet to diverge. Consequently, this mode of rotation increases the tail effectiveness at large angles of yaw but is less satisfactory in this respect than the inboard mode of rotation for other angles of yaw. This reasoning explains the favorable effect of outboard propeller rotation upon twin tail 4 when operating at an angle of sideslip of 10°. At this angle, owing to its original lateral displacement, this tail lies within the slipstream.

The data obtained in the tests indicate that for twin-engine airplanes equipped with single vertical tails and conventional right-hand propellers, the failure of a left engine will impose the more severe flight conditions. For airplanes equipped with twin vertical tails, however, the failure of a right engine should prove more critical to the fulfillment of the Army requirements. Similarly, it may be reasoned that use of propellers rotating inboard on both wings (symmetric rotation) would be advantageous for airplanes equipped with single fins both to improve tail effectiveness and to make the handling of controls similar regardless of the location of the

inoperative engine. Conversely, symmetric outboard rotation should be favorable for airplanes equipped with twin fins.

Effect of Vertical-Tail Design

Effect of vertical-tail area.- The effect of varying vertical-tail area was obtained from a study of the test data for geometrically similar tails 1, 2, and 3. The data for these tails with rudder fixed were converted to values of full-scale brake horsepower and plotted in figure 20.

The data of figure 20(a) show that increasing the vertical-tail area resulted in increases in the asymmetric power balanced by a given rudder deflection at zero angle of sideslip. These increases, however, are not directly proportional to the increase in tail (rudder) area, as might normally be expected; this lack of proportionality indicates the presence of secondary slipstream effects upon the vertical tail surfaces. Such secondary effects are probably produced by the sidewash angles generated at the tail by inflow into the slipstream jet as well as by the more direct effects of slipstream velocity. Further investigation, however, is required to establish a complete explanation of these secondary slipstream effects.

The data in figure 20(b) illustrate the favorable effect upon the asymmetric power characteristics of increasing the vertical-tail area at an angle of sideslip of 10°. These data show that, when the airplane is sideslipping, the directional stability of the vertical tail surfaces reinforces the action of the rudder control in nullifying the effects of asymmetric power, and higher values of asymmetric thrust can therefore be balanced by a given vertical-tail arrangement. The magnitude of the effects of directional stability can be obtained from a study of the curve for a rudder deflection of 0° (fig. 20(b)), which is directly indicative of the rudder-fixed directional stability. These data show that the directional stability contributed by tail 1 barely balanced the unstable yawing moments created by the yawed fuselage-wing combination. Making the tail area larger than that of tail 1 increased the directional stability, as would be expected.

The effects of increasing tail area noted in the tests with rudder fixed were also observed in the tests with rudder free. Figure 11 illustrates the influence of tail area upon the rudder-free trim characteristics of the model operating under asymmetric power. In this figure, the data indicate that freeing the rudder of tail 1 was destabilizing, as would normally be expected since the rudder type employed had a negative floating ratio. Because of the slender margin of stability associated with tail 1, the destabilizing action of freeing the rudder was sufficient to cause directional instability. Making the tail area greater than that of tail 1 increased the directional stability contributed by the tail surfaces sufficiently to overcome the destabilizing effects of the fuselage and, consequently, permitted increases in the asymmetric thrust balanced by the vertical tail surfaces.

Comparison of twin tail and single tail.- Twin tail 4 may be directly compared with tail 2 inasmuch as both tails were of the same aspect ratio and equal area. Because the twin tail was located almost directly in the slipstream, the twin tail was more effective than the single tail at zero and small angles of sideslip. Figure 21 shows that the influence of power at $\beta = 0^\circ$ made tail 4 almost as effective as tail 3, a surface of equal aspect ratio but possessing 50 percent greater area. At angles of sideslip greater than 0°, however, tail 4 was less effective than tail 2 with the rudder fixed at an angle of sideslip of 10° and with the rudder free (fig. 22). These data confirm trends noted in the past and indicate that the directional stability contributed by a twin vertical tail is less than that contributed by a single tail of the same aspect ratio and equal area. The increased directional stability achieved by use of the single tail is partly ascribed to the favorable end-plate effect of the horizontal surfaces upon the load characteristics of the vertical surfaces. In addition, the single tail has but one root juncture compared with two for the twin tail and therefore is less affected by interference effects.

It should be noted that the curves for tail 4 for rudder free (fig. 22(b)) do not pass through the origin but fall above and below it depending on the mode of propeller rotation employed. These curves indicate that reversing the propeller rotation altered the sidewash caused by the propeller sufficiently to reverse the local angle of attack of tail 4 at small angles of sideslip.

The results of the tests indicate that choice between single and twin vertical tails would depend largely upon the pilot's handling of the controls following a sudden engine failure. If the rudder control can be applied before the airplane reaches a moderately large angle of sideslip, the twin-tail design should be more suitable; otherwise, the single vertical-tail design would be preferable.

Effect of increasing aspect ratio.- The effect of increasing aspect ratio was determined from a comparison of the data obtained with tail 6, a surface of twice the aspect ratio of tail 2, with corresponding data for tails 2 and 3. These data are shown in figure 23 and indicate that doubling the aspect ratio of tail 2 has approximately the same effect as increasing the area by 50 percent at the same aspect ratio (tail 3). This effect is in close agreement with the wind-tunnel force data of reference 5, which show that doubling the aspect ratio of a surface from 1.5 to 3.0 increased the lift-curve slope from 2.2 to 3.1. For a given rudder configuration, such a change in lift-curve slope would result in an increase in total tail load, or trimming effectiveness, equivalent to that obtainable by approximately a 50-percent increase in area.

Comparison of conventional tail and all-movable tail with linked tab.- The question has been raised whether the efficient action of the all-movable tail reported in reference 6 arose largely from the "all-movable" feature or from the fact that the tail was of high aspect ratio and had the inherent advantages associated with tails of that type. For the present investigation, therefore, tests of the all-movable tail 5 were supplemented with tests of tail 7, which is identical with tail 5 except that tail 7 is of conventional - that is, fixed-fin - design.

A comparison of the effects of tails 5 and 7 upon the characteristics of the airplane operating with asymmetric power is shown in figure 24. These data indicate that the all-movable tail is markedly more effective than the conventional tail at zero sideslip with the rudder fixed and with the rudder free. At 10° sideslip and with rudder fixed, however, the all-movable tail was only slightly more effective than the conventional tail (fig. 24(a)).

These test results may be explained by use of the curves showing typical tail loads (fig. 25). These curves

show the variation of tail load with vertical-tail incidence and rudder deflection for a conventional and an all-movable tail. The tab area of the all-movable tail is assumed equal to the rudder area of the conventional tail. The variation of the load with deflection of the all-movable tail is indicated by the dashed line in figure 25. This variation is due to the linkage between the tab and the movable forward surface. The slope of the load curve is determined from the linkage ratio δ_T/i_t which, for the case investigated, was equal to 1.12. If the effect of power is ignored, the angle of attack (tail incidence) of the conventional tail at $\beta = 0^\circ$ is also zero. The rudder deflection therefore produces changes in load along a path coincidental with the zero ordinate. For example, a rudder deflection of 10° produces the tail load corresponding to the load indicated by point a. For the all-movable tail, however, a rudder deflection of 10° causes a simultaneous change in tail angle of attack and tab deflection and produces the load indicated by point b. Consequently, at zero sideslip, the all-movable tail is capable of producing much larger yawing moments with which to balance the effect of asymmetric power than the conventional tail.

At moderate angles of sideslip (10° to 15°), the conventional tail operates in the high-lift region of the lift curve of the tail and consequently produces tail loads of an order comparable with those produced by the all-movable tail. The conventional tail may conceivably produce tail loads even greater than those of the all-movable tail because the conventional tail is unrestricted in the use of rudder. The all-movable tail, however, is limited for a given linkage ratio to the rudder deflection that produces the tail incidence at maximum lift. Further deflection would cause the entire surface to stall.

In balancing the effects of asymmetric power, the superiority of the all-movable tail to the conventional tail was most marked in the rudder-free tests. This superiority can be ascribed to the fact that the hinge-moment characteristics of the all-movable tail force the entire tail to float against the wind when free (positive floating ratio) and consequently increase the directional stability of the airplane. In considering the advantages of the all-movable vertical tail over the conventional tail, it should be observed that "snaking" oscillations may be induced by control-surface friction with improperly designed tails having positive floating ratios. (See reference 6.)

Effect of rudder chord.- The effect of decreasing rudder chord is shown by the test data for tails 6 and 7 (figs. 10 and 13). These data show that, although the rudder of tail 7 had only one-half the area and one-half the chord of the rudder of tail 6, the rudder of tail 7 balanced approximately two-thirds as much asymmetric power at zero sideslip and approximately seven-eighths as much power at 10° sideslip as the rudder of tail 6. These data are in agreement with conventional trends because it is known that decreasing the rudder chord increases the yawing moment per unit rudder area.

With rudder free, tail 7 balanced a greater amount of asymmetric power than tail 6, which indicated a favorable effect of reduced rudder area upon the rudder-free directional stability. This action occurred because the rudders of tails 6 and 7 are of the type that trail with the wind and so reduce the directional stability when set free. Consequently, tail 7, because of its smaller rudder area, created smaller destabilizing moments when the rudder was set free and so balanced a greater amount of asymmetric power.

Effect of rudder deflection.- The data obtained in the tests showed that increasing the rudder deflection increased the amount of asymmetric power balanced by the vertical tails at a decreasing rate.

Effect of dorsal and ventral fins.- The data illustrating the effect of adding dorsal- and ventral-fin areas to tails 2, 3, 5, 6, and 7 are presented in figures 14 to 18. No data are presented for tail 1 because the addition of dorsal and ventral fins did not noticeably lessen the directional instability associated with this tail arrangement.

The test data indicated that the addition of auxiliary fin area increased the directional stability at large angles of yaw and thereby increased the maximum amount of asymmetric thrust balanced by the tail surfaces when the rudders were free. Increases in maximum asymmetric thrust of the order of 30 to 100 percent were observed in the tests.

The addition of ventral-fin area was generally found to be more effective than the addition of an equal amount of dorsal-fin area. The use of a combination of dorsal- and ventral-fin areas (dorsal a and ventral a) was

generally more effective than a single dorsal fin of the same total area (dorsal b).

Aileron deflections required to trim asymmetric thrust.- A representative plot of total aileron deflections required to trim the rolling moments created by asymmetric thrust is presented in figure 26. These deflections were always obtained by equal up-and-down movements of the ailerons. Calculated values are also presented in figure 26. These calculations were made by using the method presented in reference 7. The calculated lift increments created by the operating propeller were multiplied by the lateral arm of the propeller to obtain rolling moments, which were converted to aileron deflections required to trim by use of the data in figure 7.

The results presented in figure 26 show that, although the scatter was considerable, the test data agreed fairly well with the calculated values and indicated that moderately large aileron deflections would be required to maintain straight flight under asymmetric power conditions.

CONCLUSIONS

The following conclusions were drawn from trim tests of a twin-engine-airplane model operating under asymmetric power (single-engine) conditions specified by the NACA and Army Air Forces:

1. The direction of rotation of the operating propeller had an important effect upon the asymmetric power that could be balanced by a given vertical-tail design. Single vertical tails were most effective when the operating propeller was rotating inboard. Twin tails, however, were most effective when the operating propeller was rotating outboard.

2. An all-movable vertical tail of aspect ratio 3 with a linked tab was more effective than the conventional tail of the same aspect ratio and equal area in balancing asymmetric power, particularly when the rudders were free. The all-movable tail was markedly superior to the conventional vertical tail of normal aspect ratio (1.5).

3. The single vertical-tail designs generally balanced a greater amount of asymmetric power than twin vertical

tails of the same aspect ratio and equal area, particularly when the rudder was free. At small angles of sideslip, however, it was possible to balance more power by rudder deflection of the twin tails than by rudder deflection of a single tail.

4. Increasing the aspect ratio of a vertical tail resulted in increasing its trimming effectiveness under asymmetric power conditions by an amount proportional to the accompanying increase in lift-curve slope.

5. The trimming effectiveness of the vertical tail surface increased almost linearly with the vertical-tail area. Increasing rudder deflection and rudder chord increased the trimming effectiveness of the vertical tail under asymmetric conditions at a decreasing rate.

6. When the rudder was free, addition of dorsal- and ventral-fin areas increased the capacity of the vertical tail surfaces to balance asymmetric-power effects at moderate angles of sideslip.

Langley Memorial Aeronautical Laboratory
National Advisory Committee for Aeronautics
Langley Field, Va.

REFERENCES

1. Gilruth, R. R.: Requirements for Satisfactory Flying Qualities of Airplanes. NACA ACR, April 1941. (Classification changed to Restricted Oct. 1943.)

2. Anon.: Stability and Control Requirements for Airplanes. AAF Specification No. C-1815, Aug. 31, 1943.

3. Shortal, Joseph A., and Osterhout, Clayton J.: Preliminary Stability and Control Tests in the NACA Free-Flight Wind Tunnel and Correlation with Full-Scale Flight Tests. NACA TN No. 810, 1941.

4. Pitkin, Marvin: Free-Flight-Tunnel Investigation of the Effect of Mode of Propeller Rotation upon the Lateral-Stability Characteristics of a Twin-Engine Airplane Model with Single Vertical Tails of Different Size. NACA ARR No. 3J18, 1943.

5. Zimmerman, C. H.: Characteristics of Clark Y Airfoils of Small Aspect Ratios. NACA Rep. No. 431, 1932.

6. Jones, Robert T., and Kleckner, Harold F.: Theory and Preliminary Flight Tests of an All-Movable Vertical Tail Surface. NACA ARR, Jan. 1943.

7. Pass, H. R.: Wind-Tunnel Study of the Effects of Propeller Operation and Flap Deflection on the Pitching Moments and Elevator Hinge Moments of a Single-Engine Pursuit-Type Airplane. NACA ARR, July 1942.

TABLE I.- INDEX TO FIGURES

Figure	Description	Remarks
1	Photographs of test model mounted on trim stand in Langley free-flight tunnel	Model with tail 2
2	Sketch of test model mounted on trim stand, which permitted freedom in yaw and roll, in Langley free-flight tunnel	
3	Three-view drawing of $\frac{1}{20}$-scale twin-engine model tested in Langley free-flight tunnel with asymmetric power	
4	Photograph of twin-engine model used in trim tests in Langley free-flight tunnel	Model with tail 2
5	Plan-form and dimensional characteristics of seven vertical tails tested on a $\frac{1}{20}$-scale model of a twin-engine airplane in the Langley free-flight tunnel	
6	Various fin arrangements tested with vertical tails on a $\frac{1}{20}$-scale model of a twin-engine airplane in the Langley free-flight tunnel	

Figure		Test specifications	Test condition	Tail arrangement			Operating-propeller rotation[1]	Curve	Remarks
				Tail	Dorsal	Ventral			
7		----------	---------	2	------	-------	Propeller off	C_l against δ_a	Aileron calibration
8	a	NACA ($\beta = 0^\circ$)	Rudder fixed	1 to 3	------	-------	Inboard and outboard	T_c against δ_r	Directional-control run
	b	NACA ($\beta = 10^\circ$)	Rudder fixed	1 to 3	------	-------	--------do---------	T_c against δ_r	Do.
9	a	NACA ($\beta = 0^\circ$)	Rudder fixed	4	------	-------	--------do---------	T_c against δ_r	Do.
	b	Army ($\beta = 10^\circ$)	Rudder fixed	4	------	-------	--------do---------	T_c against δ_r	Do.
10	a	NACA ($\beta = 0^\circ$)	Rudder fixed	5 to 7	------	-------	--------do---------	T_c against δ_r	Do.
	b	Army ($\beta = 10^\circ$)	Rudder fixed	5 to 7	------	-------	--------do---------	T_c against δ_r	Do.
11	a	NACA (Rudder free)	Rudder free	1 to 3	------	-------	Outboard	T_c against β	Directional-stability run
	b	NACA (Rudder free)	Rudder free	1 to 3	------	-------	Inboard	T_c against β	Do.
12	a	NACA (Rudder free)	Rudder free	4	------	-------	Outboard	T_c against β	Do.
	b	NACA (Rudder free)	Rudder free	4	------	-------	Inboard	T_c against β	Do.
13	a	NACA (Rudder free)	Rudder free	5 to 7	------	-------	Outboard	T_c against β	Do.
	b	NACA (Rudder free)	Rudder free	5 to 7	------	-------	Inboard	T_c against β	Do.
14	a	NACA (Rudder free)	Rudder free	2	All combinations[2]		Outboard	T_c against β	Effect of dorsal- and ventral-fin area
	b	NACA (Rudder free)	Rudder free	2	------do------		Inboard	T_c against β	Do.
15	a	NACA (Rudder free)	Rudder free	3	------do------		Outboard	T_c against β	Do.
	b	NACA (Rudder free)	Rudder free	3	------do------		Inboard	T_c against β	Do.

[1]Right propeller operative.

[2]Combinations tested are tail alone, dorsal a, dorsal and ventral a, ventral a, dorsal b.

TABLE I. - INDEX TO FIGURES - Concluded

Figure		Test specifications	Test condition	Tail arrangement			Operating-propeller rotation[1]	Curve	Remarks
				Tail	Dorsal	Ventral			
16	a	NACA (Rudder free)	Rudder free	5	Tail alone, dorsal a, dorsal e and ventral a		Outboard	T_c against β	Effect of dorsal- and ventral-fin area
	b	NACA (Rudder free)	Rudder free	5	All combinations[2]		Inboard	T_c against β	Do.
17	a	NACA (Rudder free)	Rudder free	6	-----do-------		Outboard	T_c against β	Do.
	b	NACA (Rudder free)	Rudder free	6	-----do-------		Inboard	T_c against β	Do.
18	a	NACA (Rudder free)	Rudder free	7	-----do-------		Outboard	T_c against β	Do.
	b	NACA (Rudder free)	Rudder free	7	-----do-------		Inboard	T_c against β	Do.
19	a	NACA (β = 0°)	Rudder fixed	1 to 7	------	-------	Inboard and outboard	bhp for δ_r = 20°	Effect of mode of rotation
	b	Army (β = 10°)	Rudder fixed	1 to 7	------	-------	--------do---------	bhp for δ_r = 20°	Do.
	c	NACA (Rudder free)	Rudder free	1 to 7	------	-------	--------do---------	bhp for 10°<β<12°	Asymmetric power balanced at verge of directional divergence
20	a	NACA (β = 0°)	Rudder fixed	1 to 3	------	-------	Outboard	bhp against tail area	Curves of various rudder deflections
	b	Army (β = 10°)	Rudder fixed	1 to 3	------	-------	--------do---------	-----do-----	Do.
21	a	NACA (β = 0°)	Rudder fixed	2 to 4	------	-------	Inboard	bhp against δ_r	Comparison single and twin tail
	b	NACA (β = 0°)	Rudder fixed	2 to 4	------	-------	Outboard	bhp against δ_r	Do.
22	a	Army (β = 10°)	Rudder fixed	2, 4	------	-------	Inboard and outboard	bhp against δ_r	Do.
	b	NACA (Rudder free)	Rudder free	2, 4	------	-------	--------do---------	bhp against β	Do.
23	a	NACA (β = 0°)	Rudder fixed	2, 3, 6	------	-------	Inboard	bhp against δ_r	Effect of aspect ratio
	b	NACA (Rudder free)	Rudder free	2, 3, 6	------	-------	--------do---------	bhp against β	Do.
24	a	NACA (β=0°) Army (β=10°)	Rudder fixed	5, 7	------	-------	Outboard	bhp against δ_r	Comparison of all-movable and conventional tail
	b	NACA (Rudder free)	Rudder free	5, 7	------	-------	--------do---------	bhp against β	Do.
25		----------	---------	----	------	-------	-------------------	Tail load against i_t	Illustrative of principle of all-movable tail
26		----------	---------	----	------	-------	Inboard and outboard	T_c against δ_a	Aileron deflections required to trim

[1]Right propeller operative.

[2]Combinations tested are tail alone, dorsal a, dorsal and ventral a, ventral a, dorsal b.

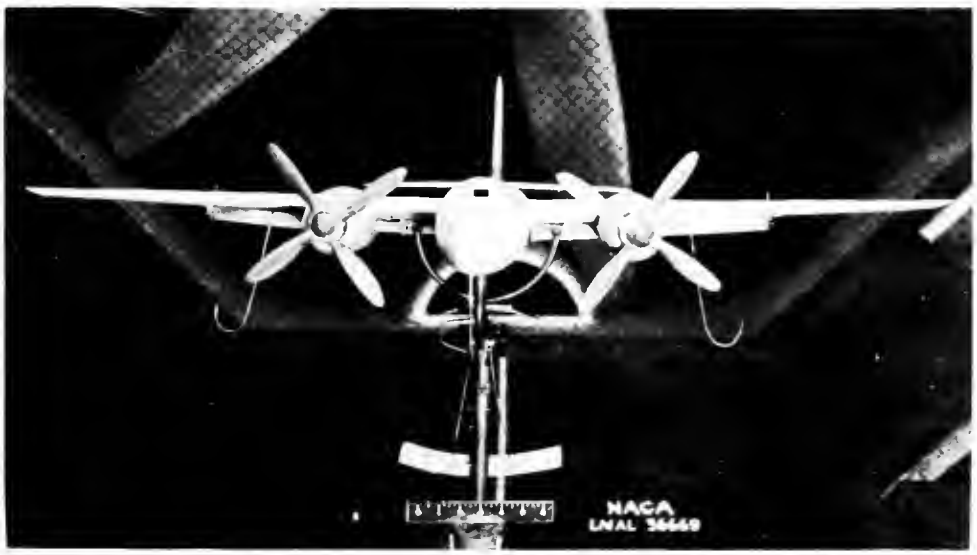

Figure 1.- Test model mounted on trim stand in Langley free-flight tunnel.

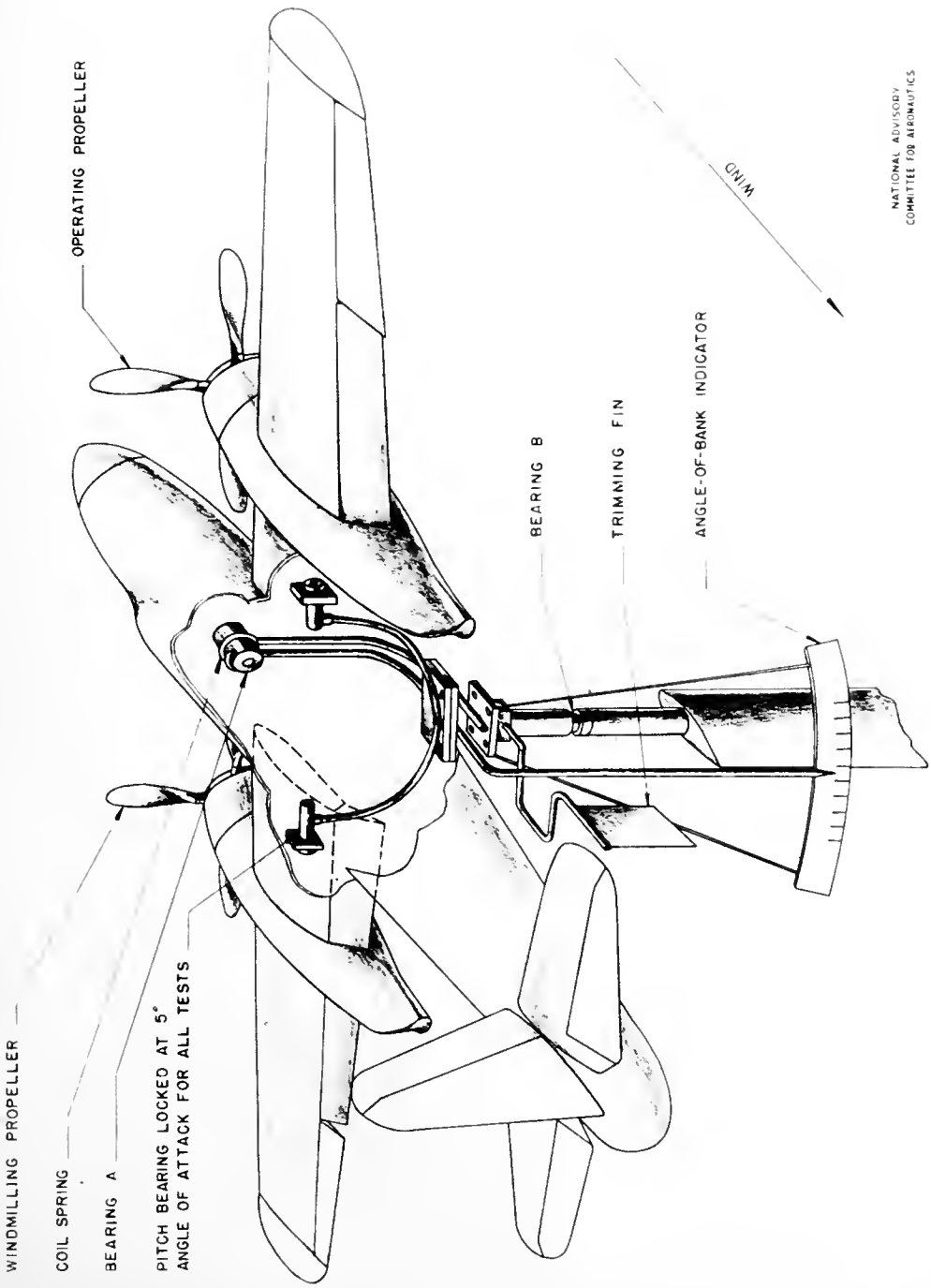

FIGURE 2.- TEST MODEL MOUNTED ON TRIM STAND IN LANGLEY FREE-FLIGHT TUNNEL. MODEL HAS FREEDOM IN YAW AND ROLL.

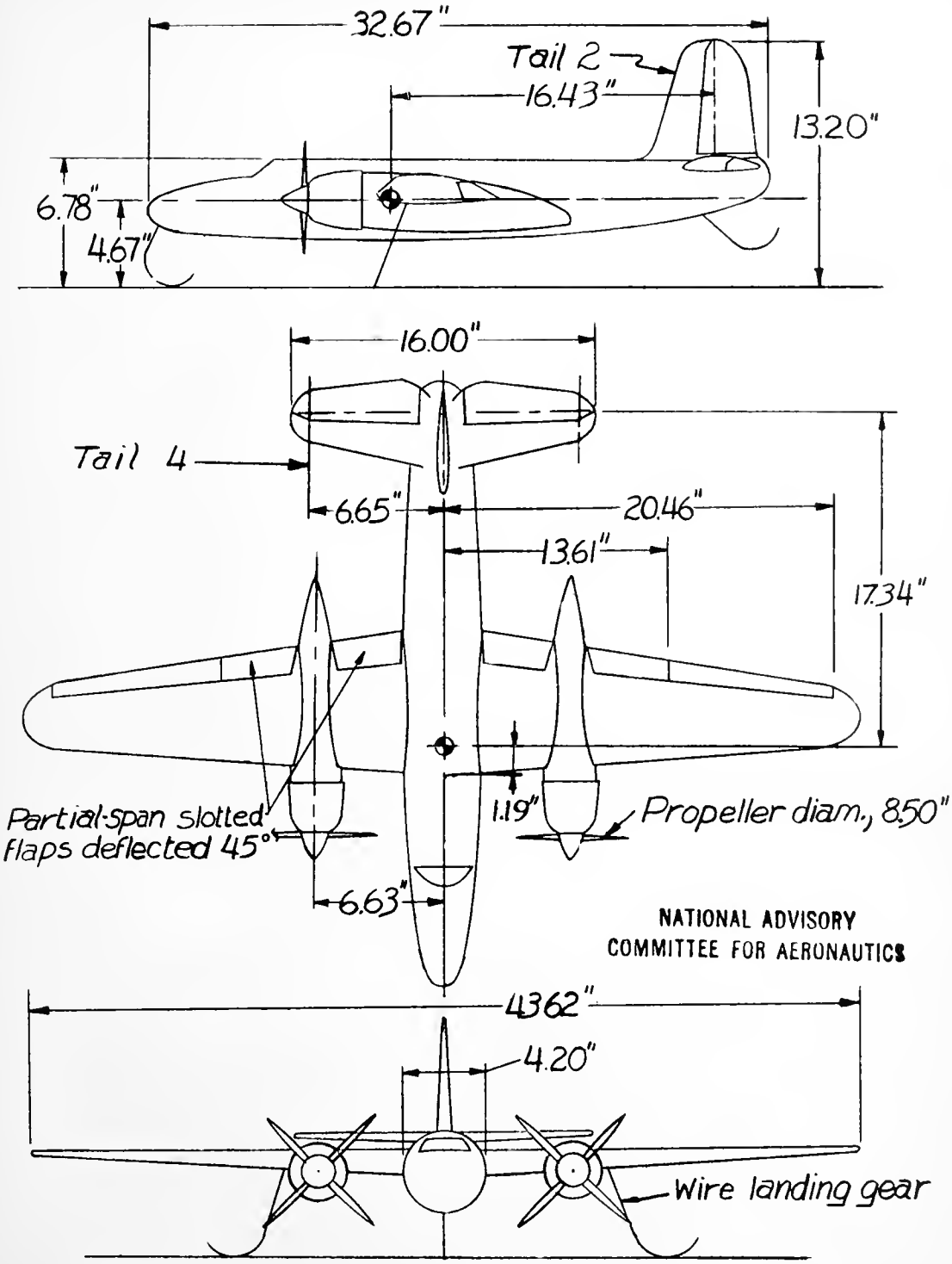

Figure 3.- Three-view drawing of 1/20-scale twin-engine model as tested in Langley free-flight tunnel with asymmetric power.

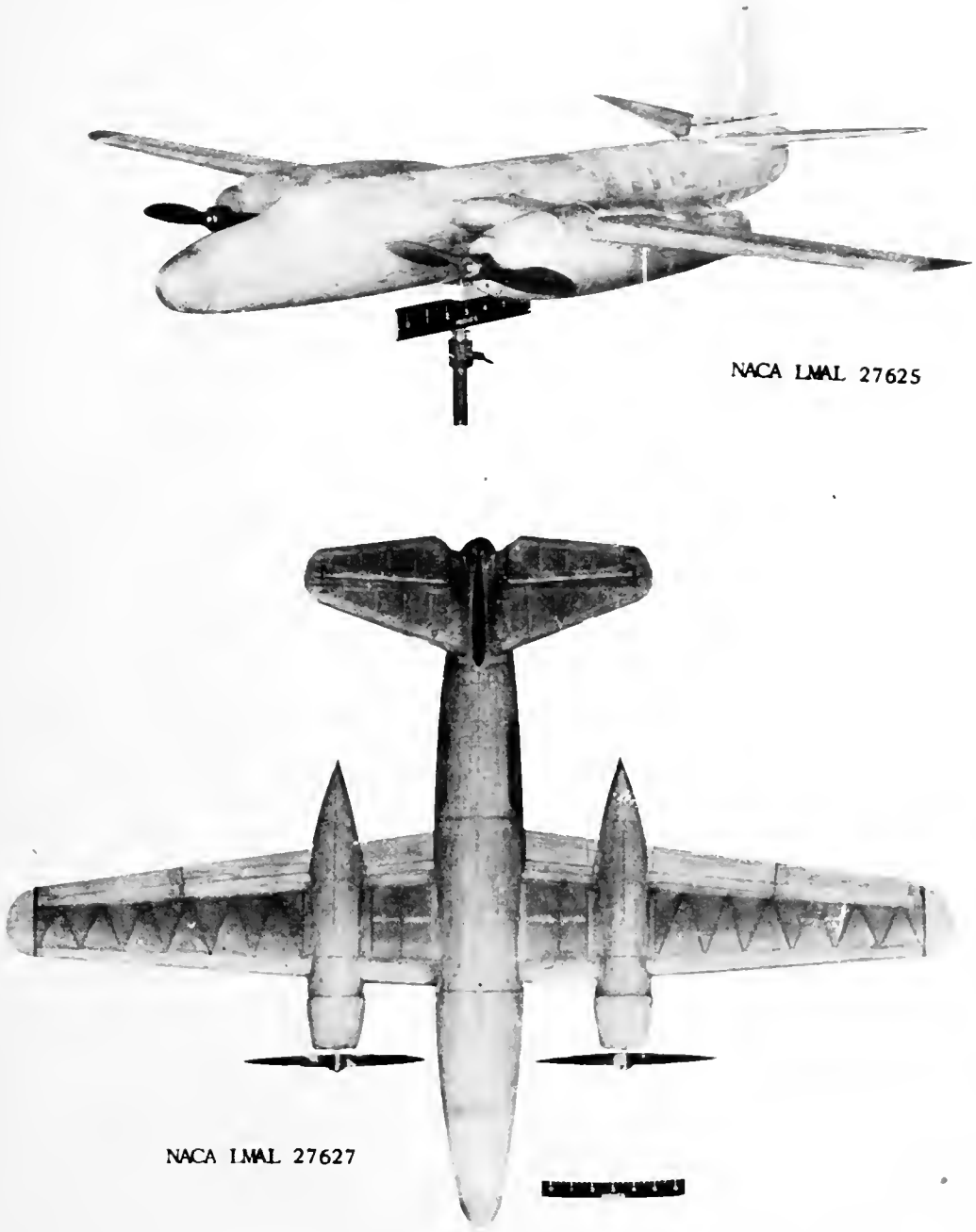

Figure 4.- Twin-engine model of B-28 airplane used in trim tests in Langley free-flight tunnel.

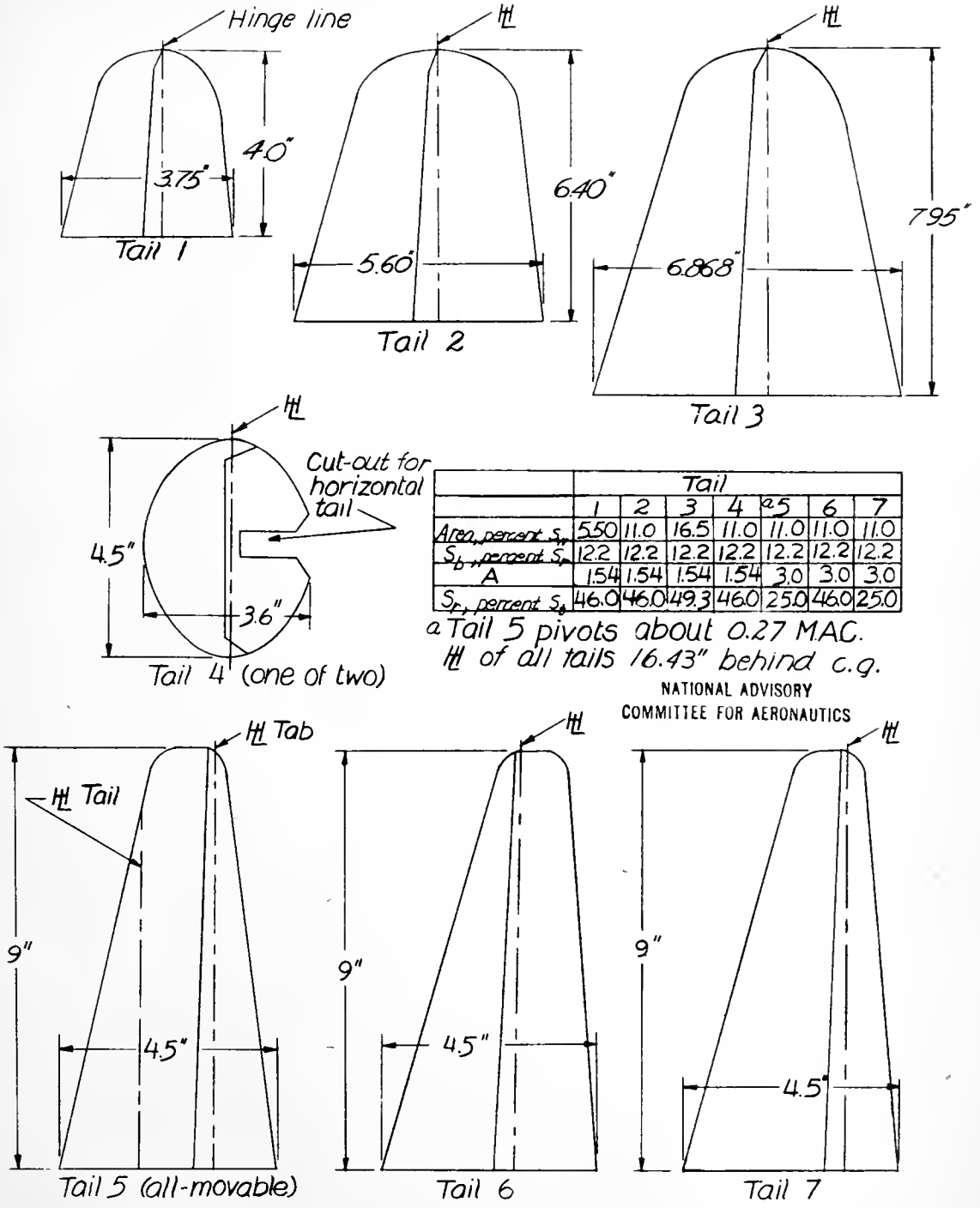

	Tail						
	1	2	3	4	[a]5	6	7
Area, percent S_v	5.50	11.0	16.5	11.0	11.0	11.0	11.0
S_b, percent S_v	12.2	12.2	12.2	12.2	12.2	12.2	12.2
A	1.54	1.54	1.54	1.54	3.0	3.0	3.0
S_r, percent S_v	46.0	46.0	49.3	46.0	25.0	46.0	25.0

[a] Tail 5 pivots about 0.27 MAC. HL of all tails 16.43" behind c.g.

Figure 5.- Plan-form and dimensional characteristics of seven vertical tails tested on a 1/20-scale model of a twin-engine airplane in the Langley free-flight tunnel.

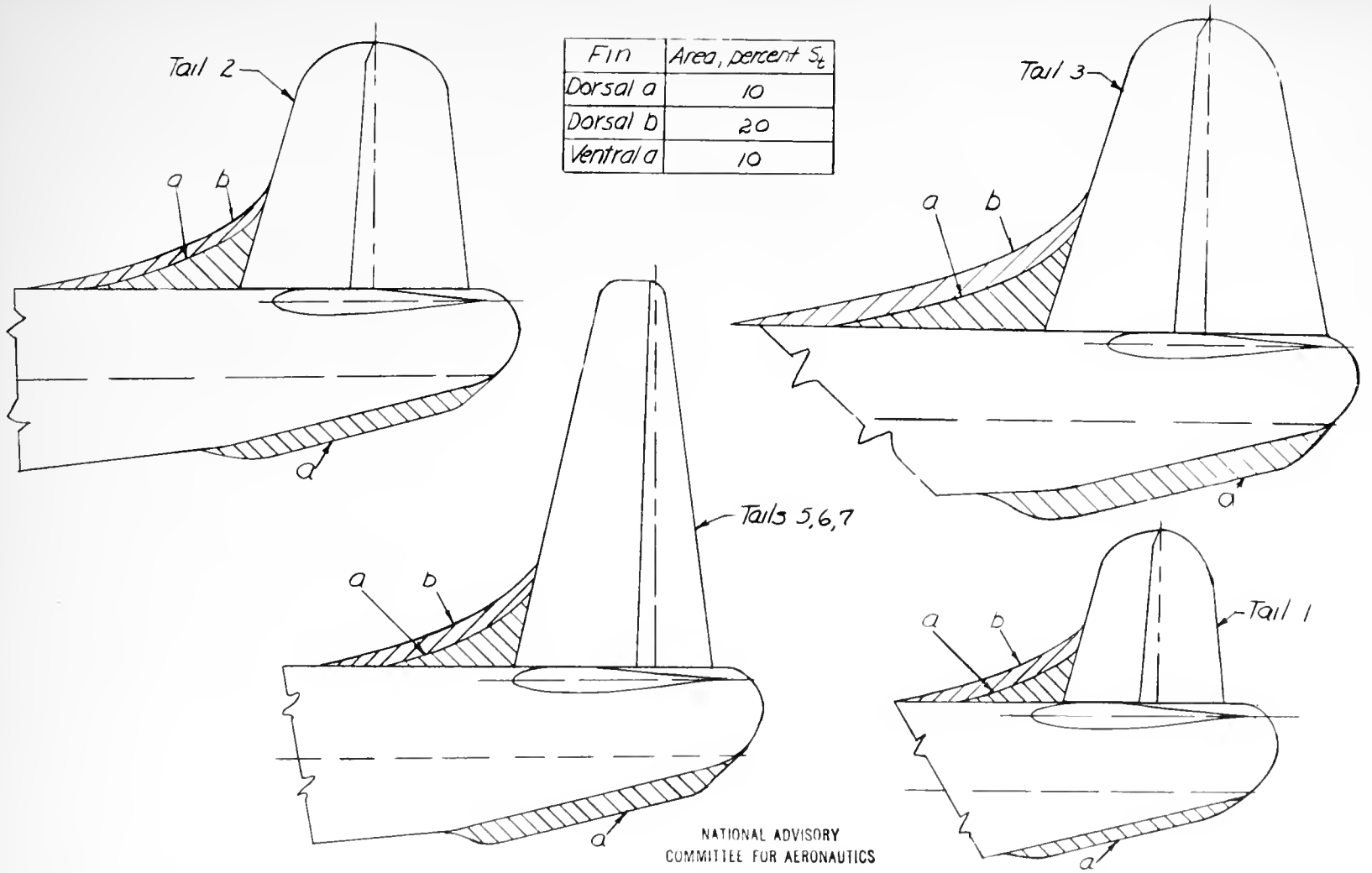

Fin	Area, percent S_t
Dorsal a	10
Dorsal b	20
Ventral a	10

Figure 6.- Various fin arrangements tested with vertical tails on 1/20-scale model of a twin-engine airplane in the Langley free-flight tunnel.

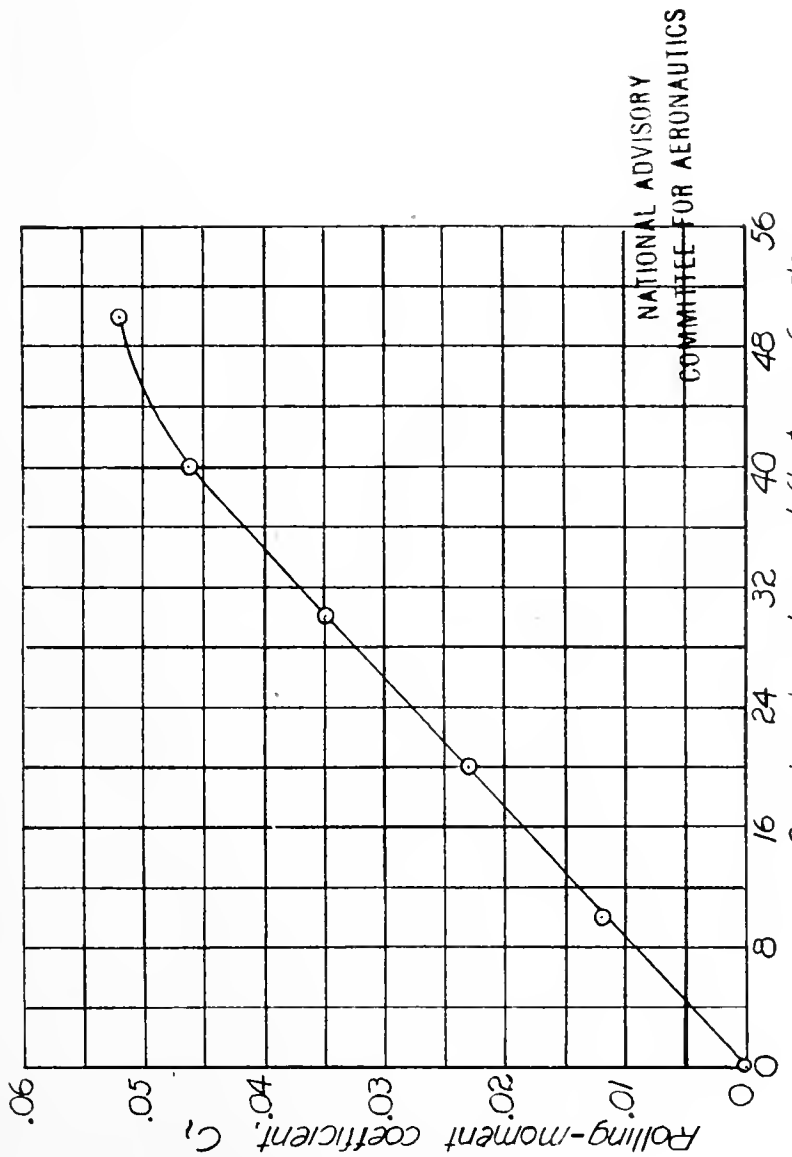

Figure 7. - Rolling-moment coefficients created by ailerons installed on test model in free-flight-tunnel investigation of asymmetric-power effects.

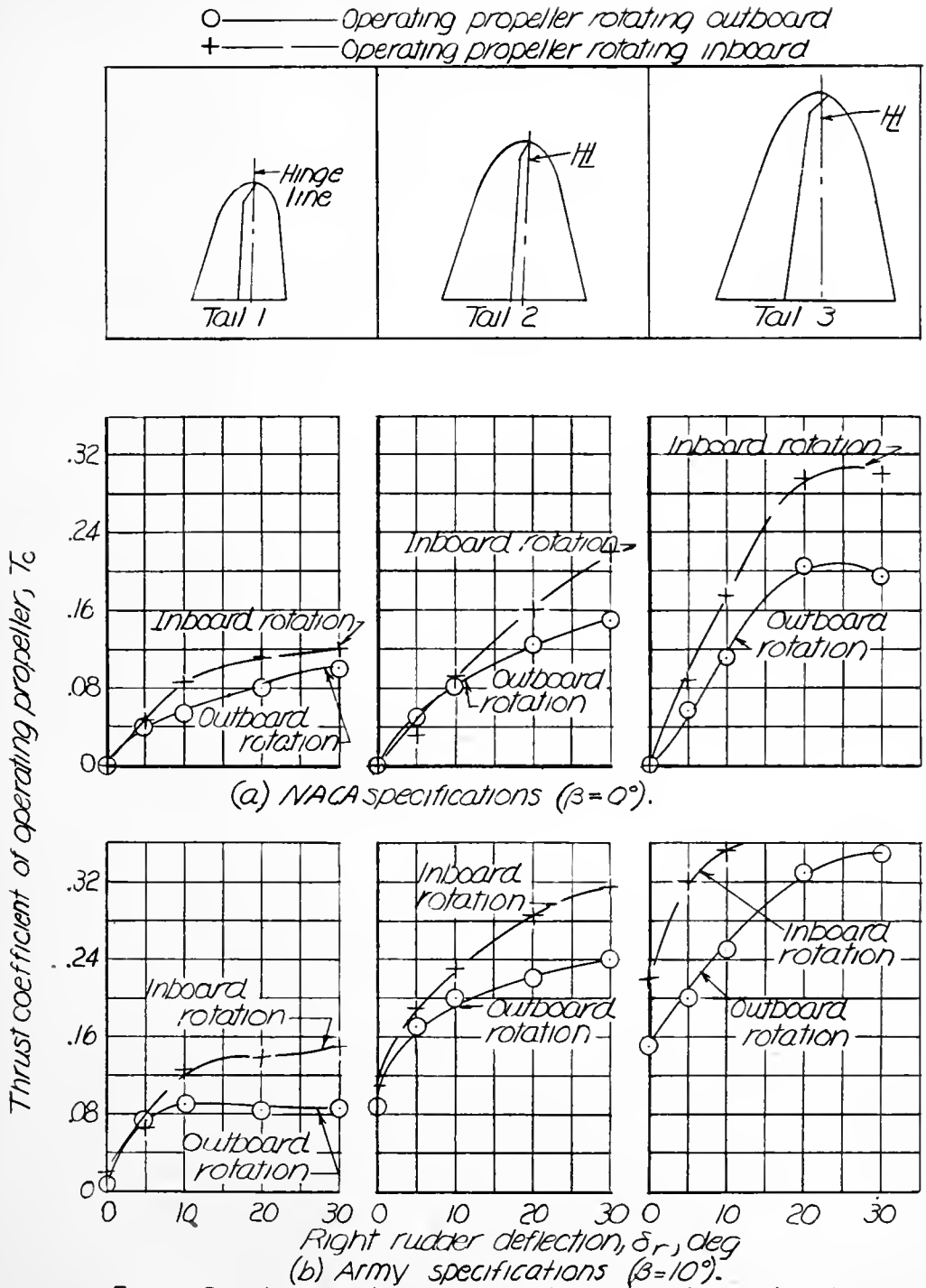

Figure 8.- Asymmetric-power characteristics of a twin-engine-airplane model equipped with vertical-tail designs 1, 2, and 3. δ_a such that the rolling moments equal 0; $\delta_f = 45°$; $\delta_e = 0°$; $\alpha = 5°$; left propeller windmilling; rudder fixed.

NATIONAL ADVISORY COMMITTEE FOR AERONAUTICS

○——— Operating propeller rotating outboard
+——— Operating propeller rotating inboard

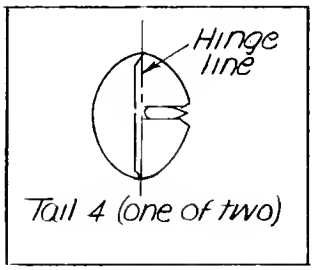

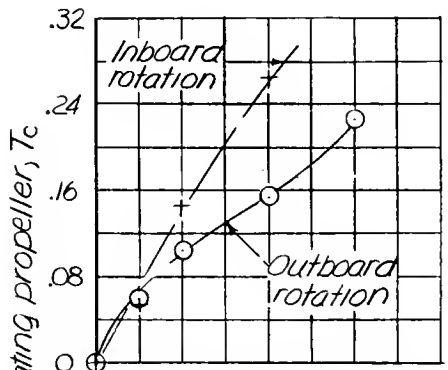

(a) NACA specifications ($\beta = 0°$).

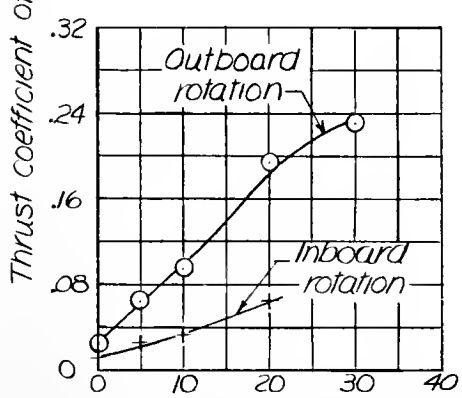

(b) Army specifications ($\beta = 10°$).

Figure 9.- Asymmetric-power characteristics of a twin-engine-airplane model equipped with vertical-tail design 4. δ_a such that the rolling moments equal 0, $\delta_f = 45°$; $\delta_e = 0°$; $\alpha = 5°$; left propeller windmilling; rudder fixed.

NATIONAL ADVISORY
COMMITTEE FOR AERONAUTICS

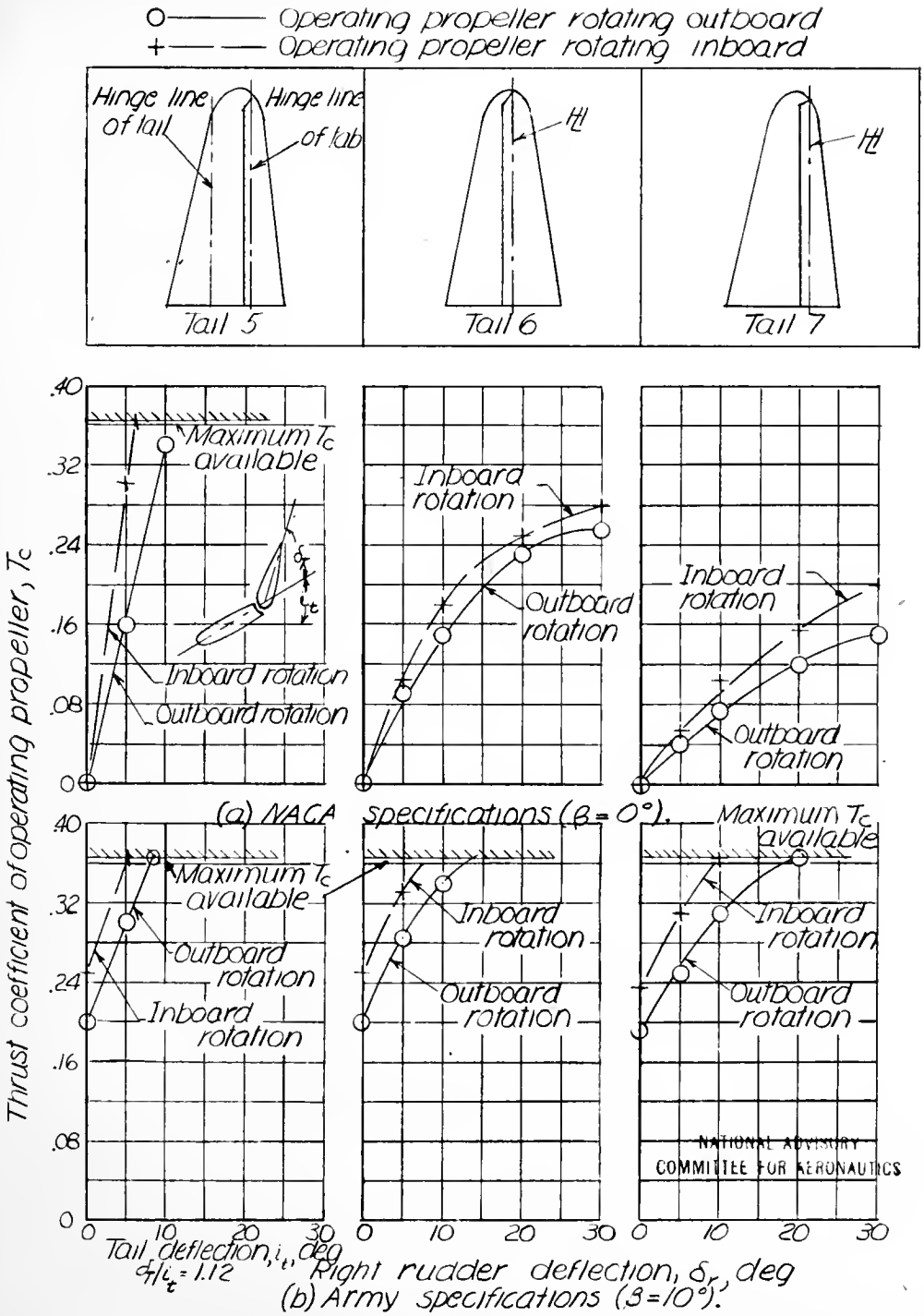

Figure 10.- Asymmetric-power characteristics of a twin-engine-airplane model equipped with vertical-tail designs 5, 6, and 7. δ_a such that the rolling moments equal 0; $\delta_f = 45°$; $\delta_e = 0°$; $\alpha = 5°$; left propeller windmilling; rudder fixed.

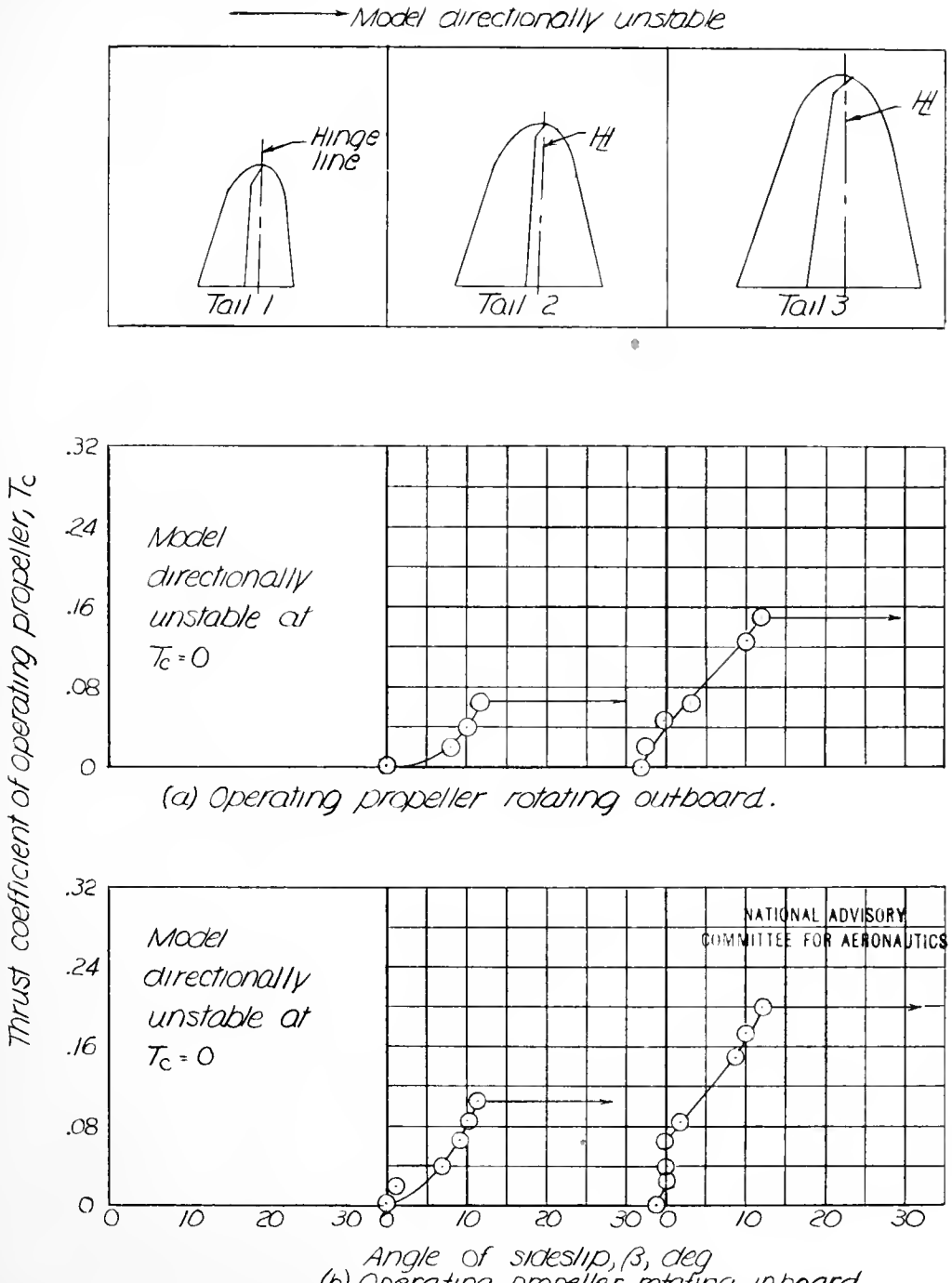

Figure 11.-Asymmetric-power characteristics of a twin-engine-airplane model equipped with vertical-tail designs 1, 2, and 3. δ_a such that the rolling moments equal 0; $\delta_r = 45°$; $\delta_e = 0°$; $\alpha = 5°$; left propeller windmilling; rudder free.

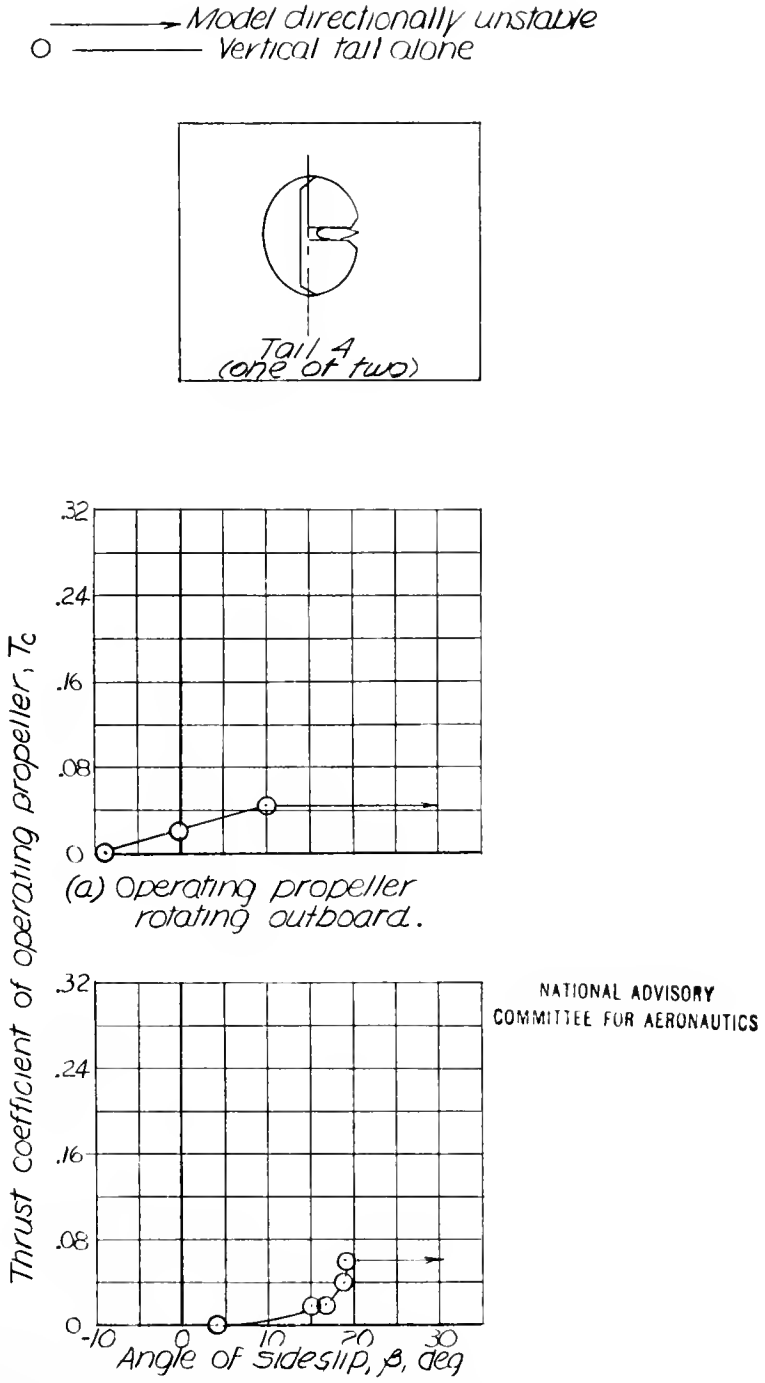

Figure 12.- Asymmetric-power characteristics of a twin-engine-airplane model equipped with vertical-tail design 4. δ_a such that the rolling moments equal 0; $\delta_f = 45°$; $\delta_e = 0°$; $\alpha = 5°$; left propeller windmilling; rudder free.

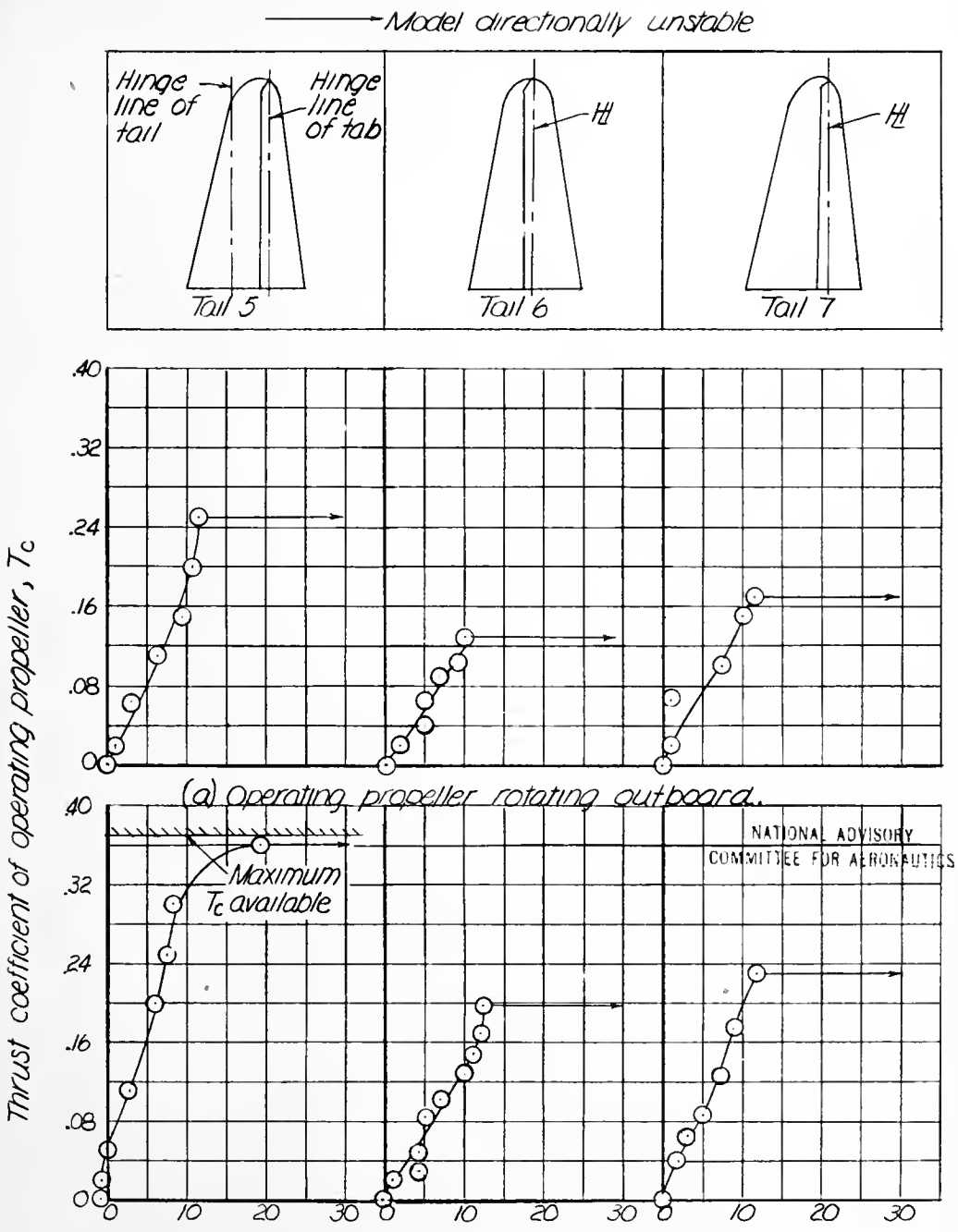

Figure 13.--Asymmetric-power characteristics of a twin-engine-airplane model equipped with vertical-tail designs 5, 6, and 7. C_a such that the rolling moments equal 0; δ_f=45; δ_e=0°; α=5°; left propeller windmilling; rudder free.

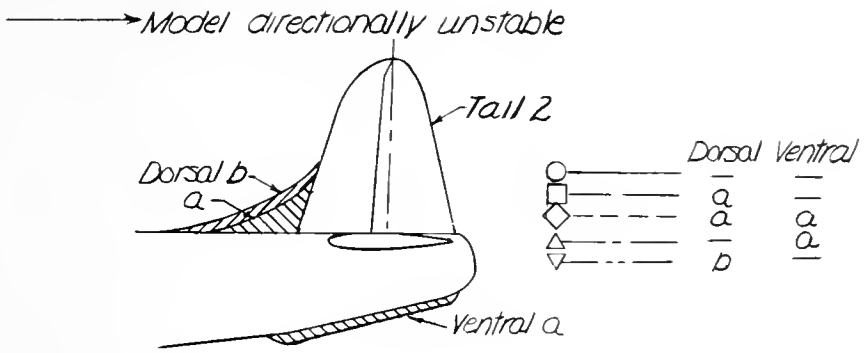

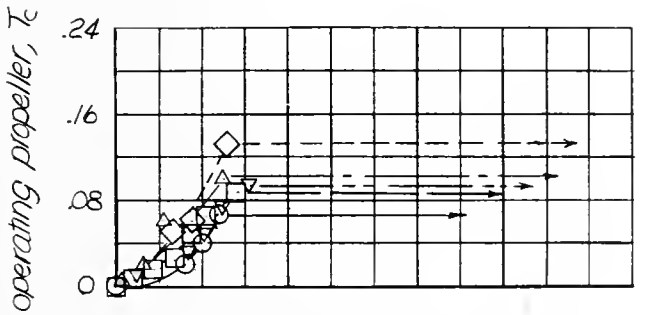

(a) Operating propeller rotating outboard.

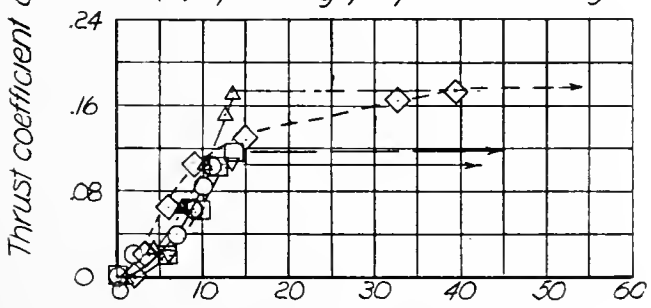

(b) Operating propeller rotating inboard.

Figure 14.- Effect of dorsal- and ventral-fin areas upon the asymmetric-power characteristics of a twin-engine-airplane model equipped with vertical-tail design 2. δ_a such that the rolling moments equal 0; $\delta_f = 45°$; $\delta_e = 0°$; $\alpha = 5°$; left propeller windmilling; rudder free.

NATIONAL ADVISORY
COMMITTEE FOR AERONAUTICS

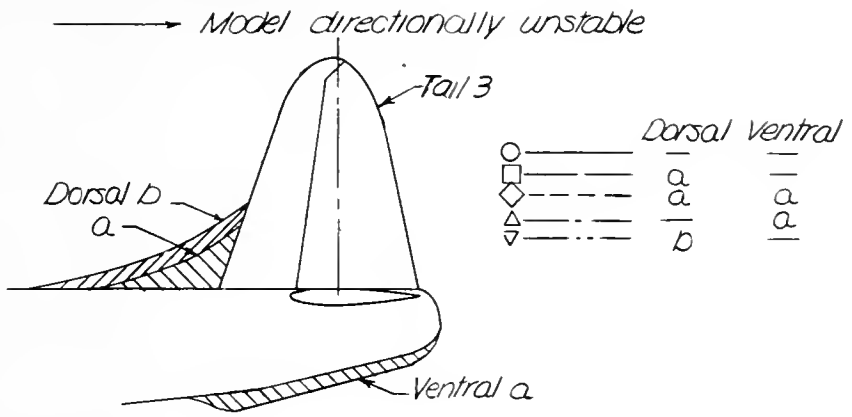

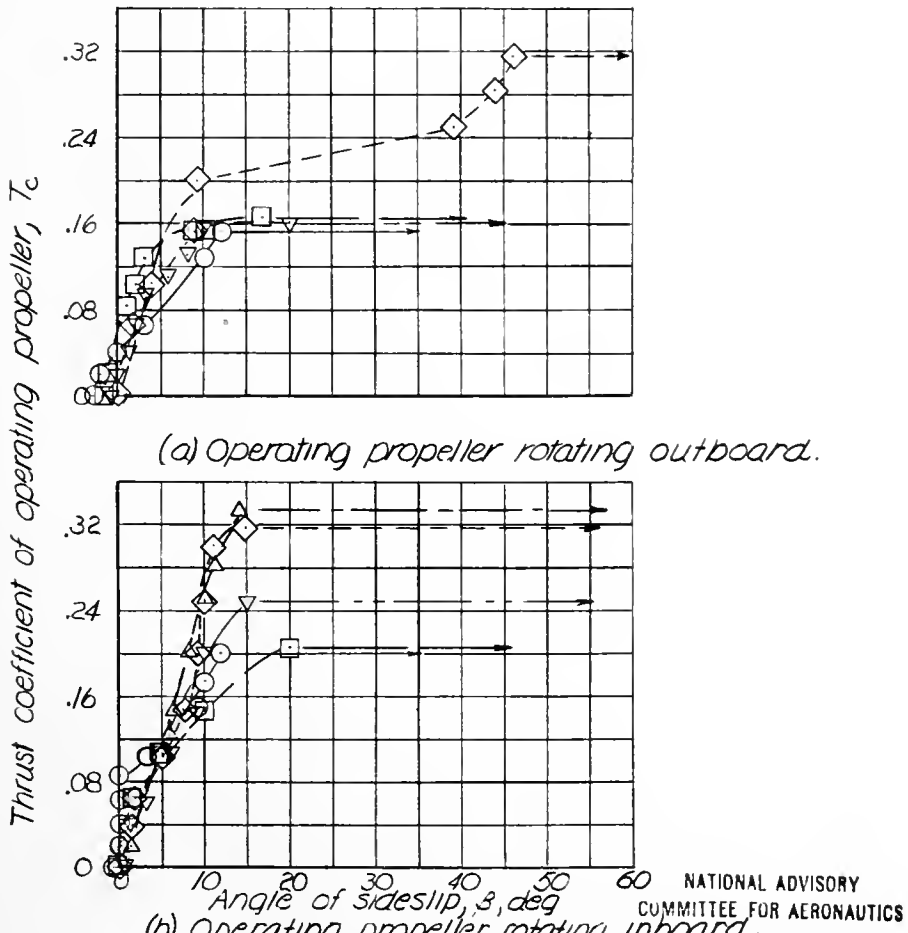

(a) Operating propeller rotating outboard.

(b) Operating propeller rotating inboard.

Figure 15 .- Effect of dorsal- and ventral-fin areas upon the asymmetric-power characteristics of a twin-engine-airplane model equipped with vertical-tail design 3. δ_a such that the rolling moments equal 0; $\delta_f = 45^\circ$; $\delta_e = 0^\circ$; $\alpha_c = 5^\circ$; left propeller windmilling; rudder free.

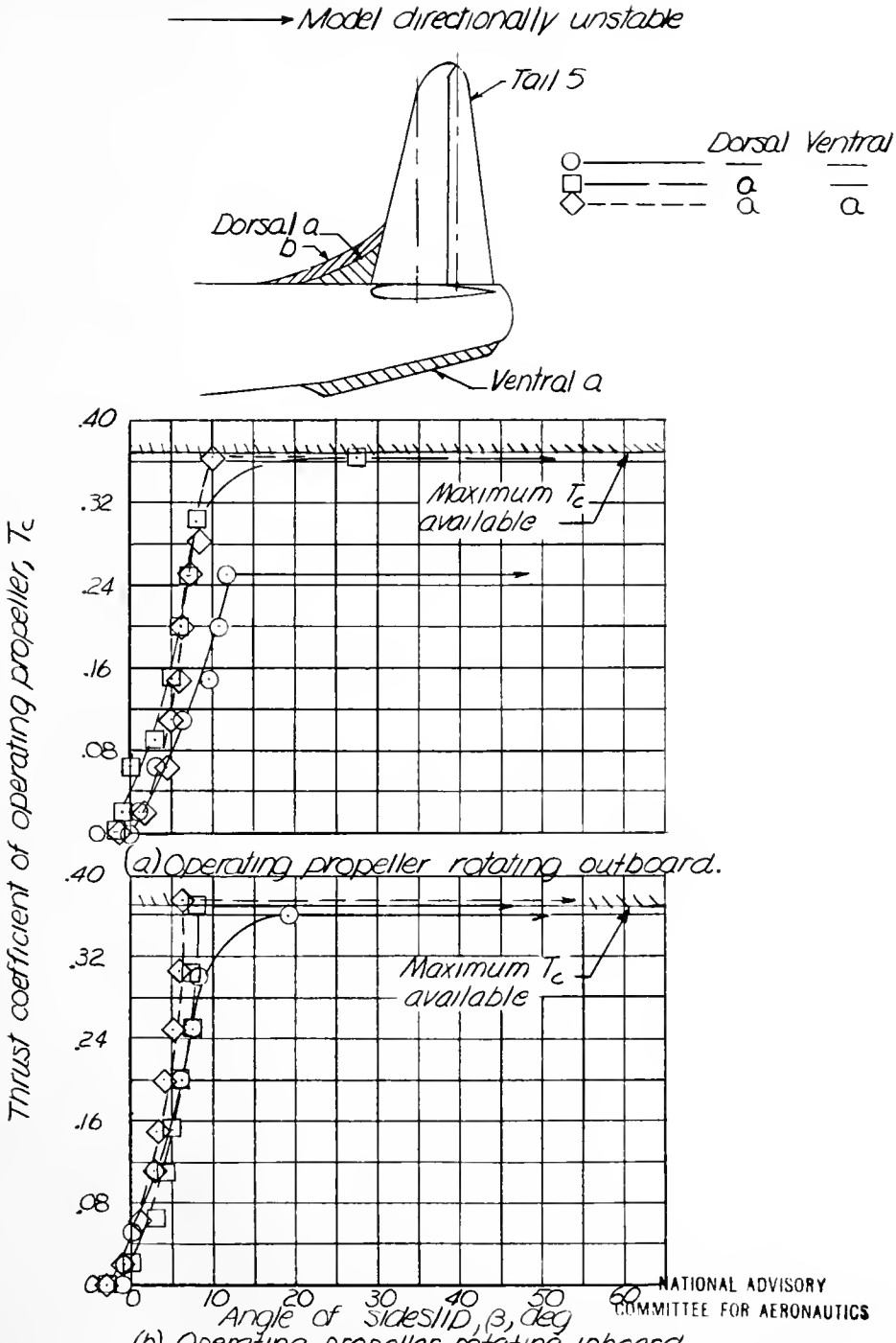

Figure 16.- Effect of dorsal- and ventral-fin areas upon the asymmetric-power characteristics of a twin-engine-airplane model equipped with vertical-tail design 5. δ_a such that the rolling moments equal 0; $\delta_f = 45°$; $\delta_e = 0°$; $\alpha = 5°$; left propeller windmilling; rudder free.

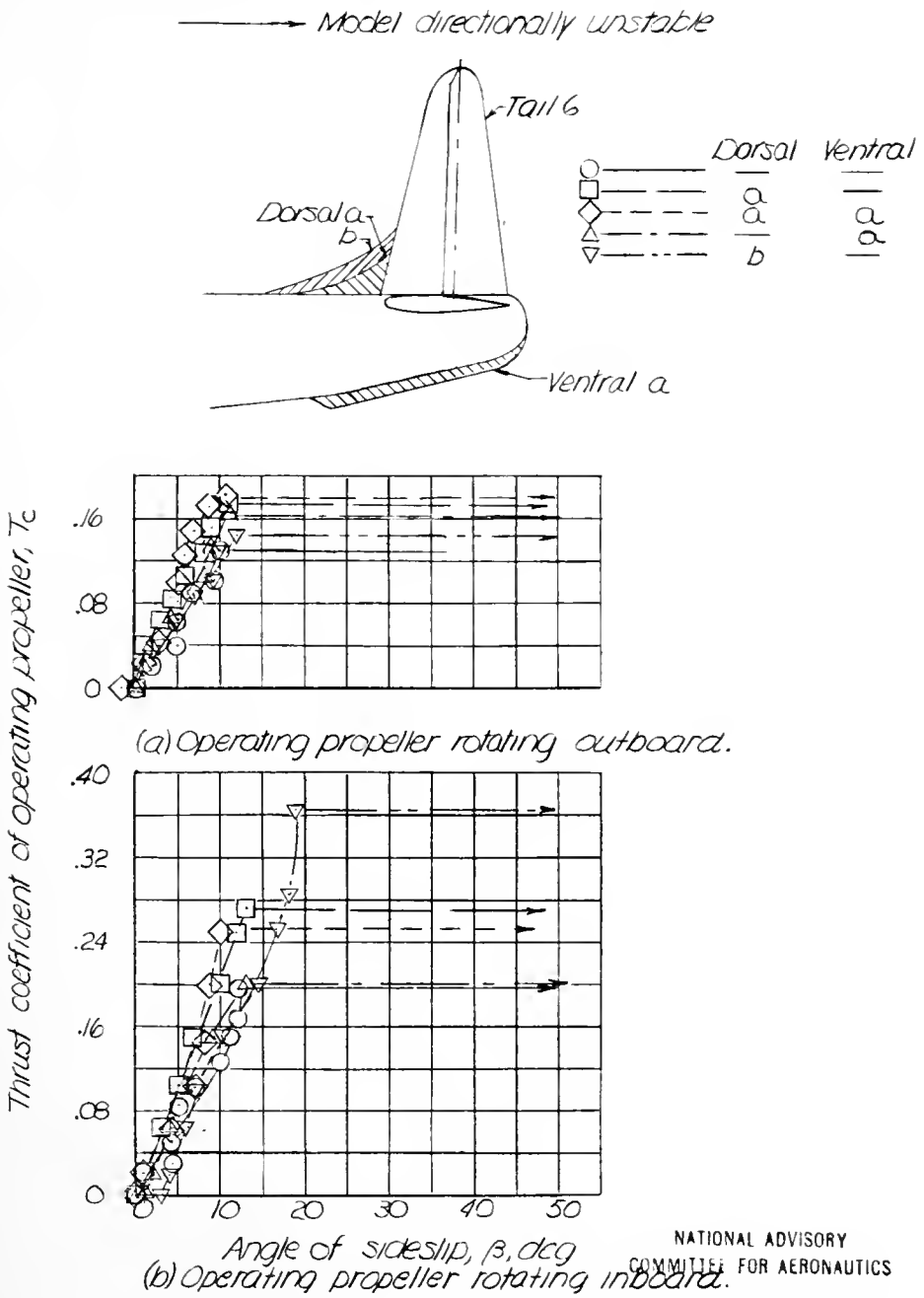

Figure 17.-Effect of dorsal- and ventral-fin areas upon the asymmetric-power characteristics of a twin-engine-airplane model equipped with vertical-tail design 6. δ_a such that the rolling moments equal 0; $\delta_f = 45°$; $\delta_e = 0°$; $\alpha = 5°$; left propeller windmilling; rudder free.

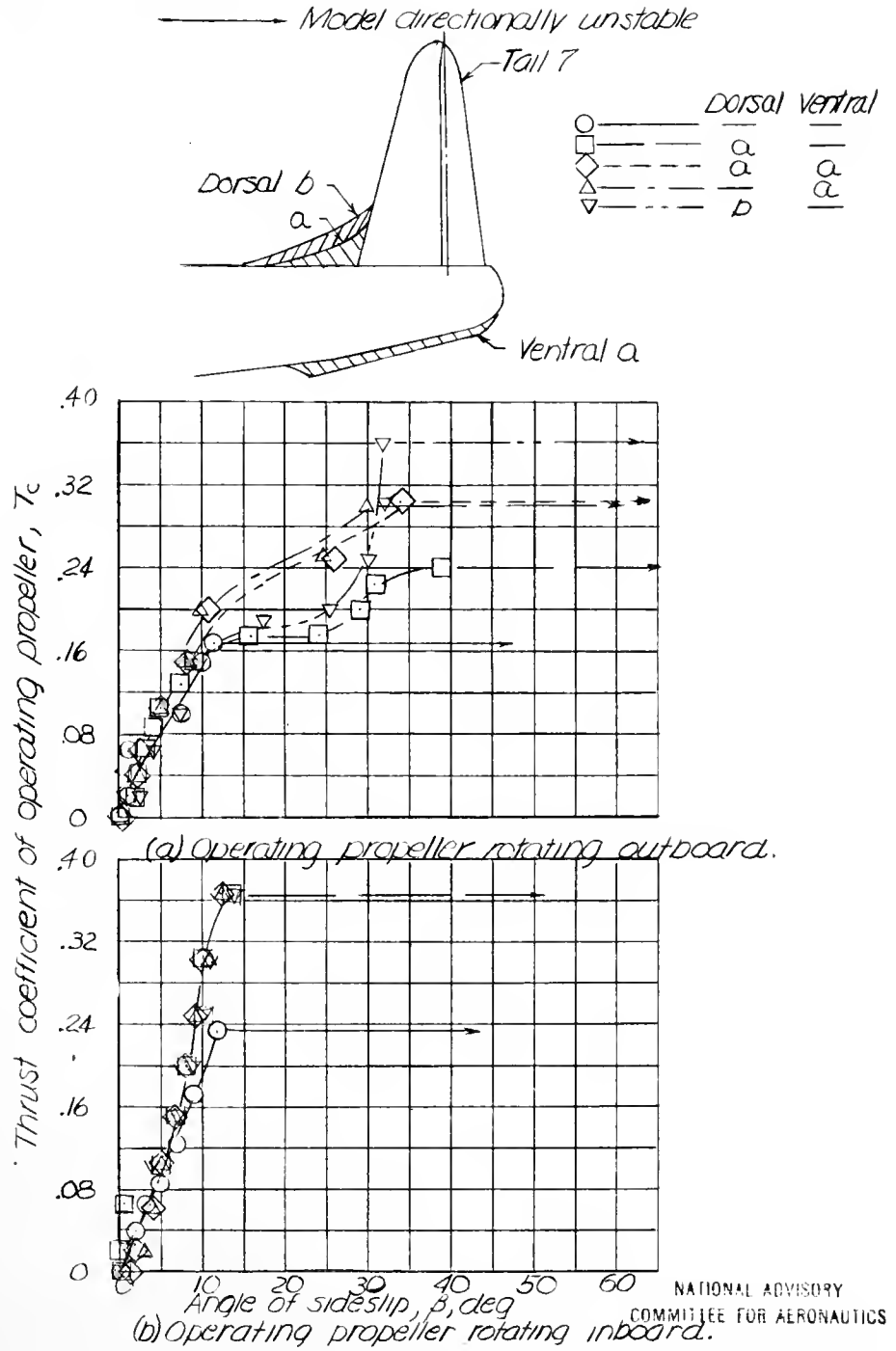

Figure 18.- Effect of dorsal and ventral fin areas upon the asymmetric-power characteristics of a twin-engine airplane model equipped with vertical-tail design 7. δ_a such that the rolling moments equal 0; $\delta_f = 45°$; $\delta_e = 0°$; $\alpha = 5°$; left propeller windmilling; rudder free.

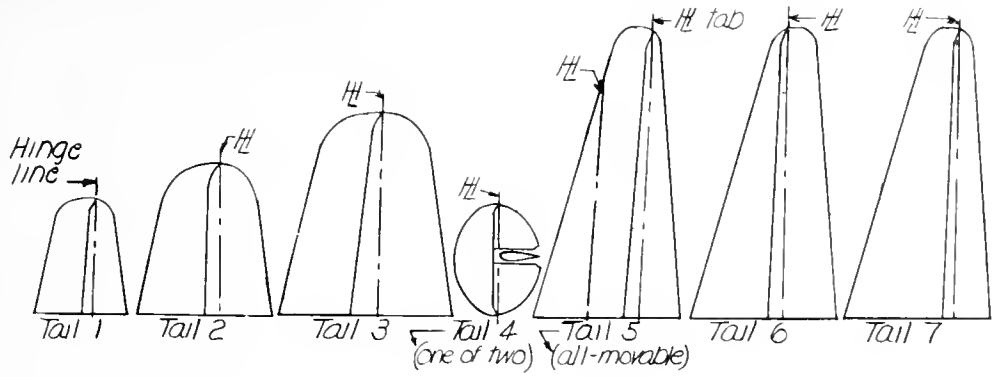

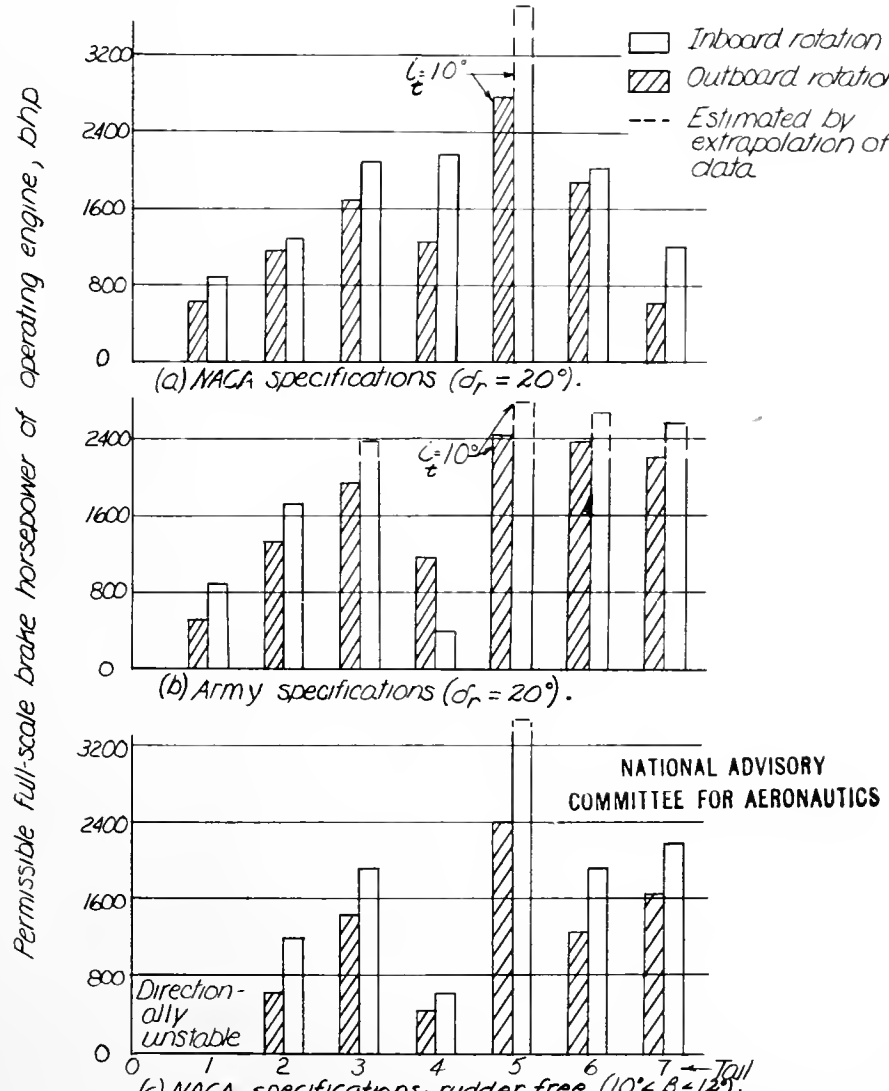

Figure 19.-Effect of mode of propeller rotation upon the permissible asymmetric brake horsepower, calculated from test data for the North American B-28 airplane operating on one engine under NACA and Army flight specifications.

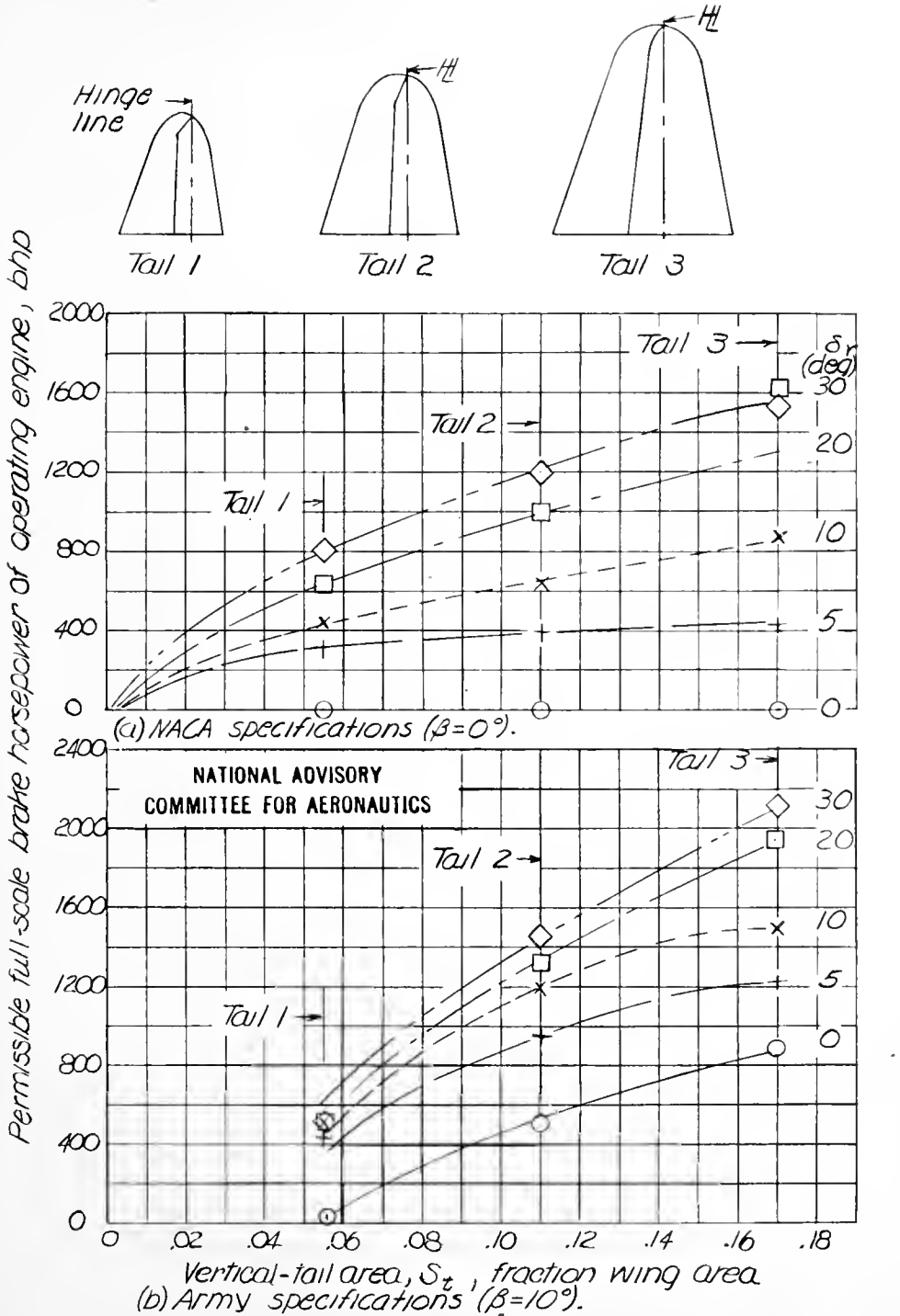

Figure 20.-Effect of vertical-tail area and rudder deflection upon the permissible brake horsepower, calculated from model test data, for the North American B-28 airplane operating on one engine under NACA and Army flight specifications. Operating propeller rotating outboard.

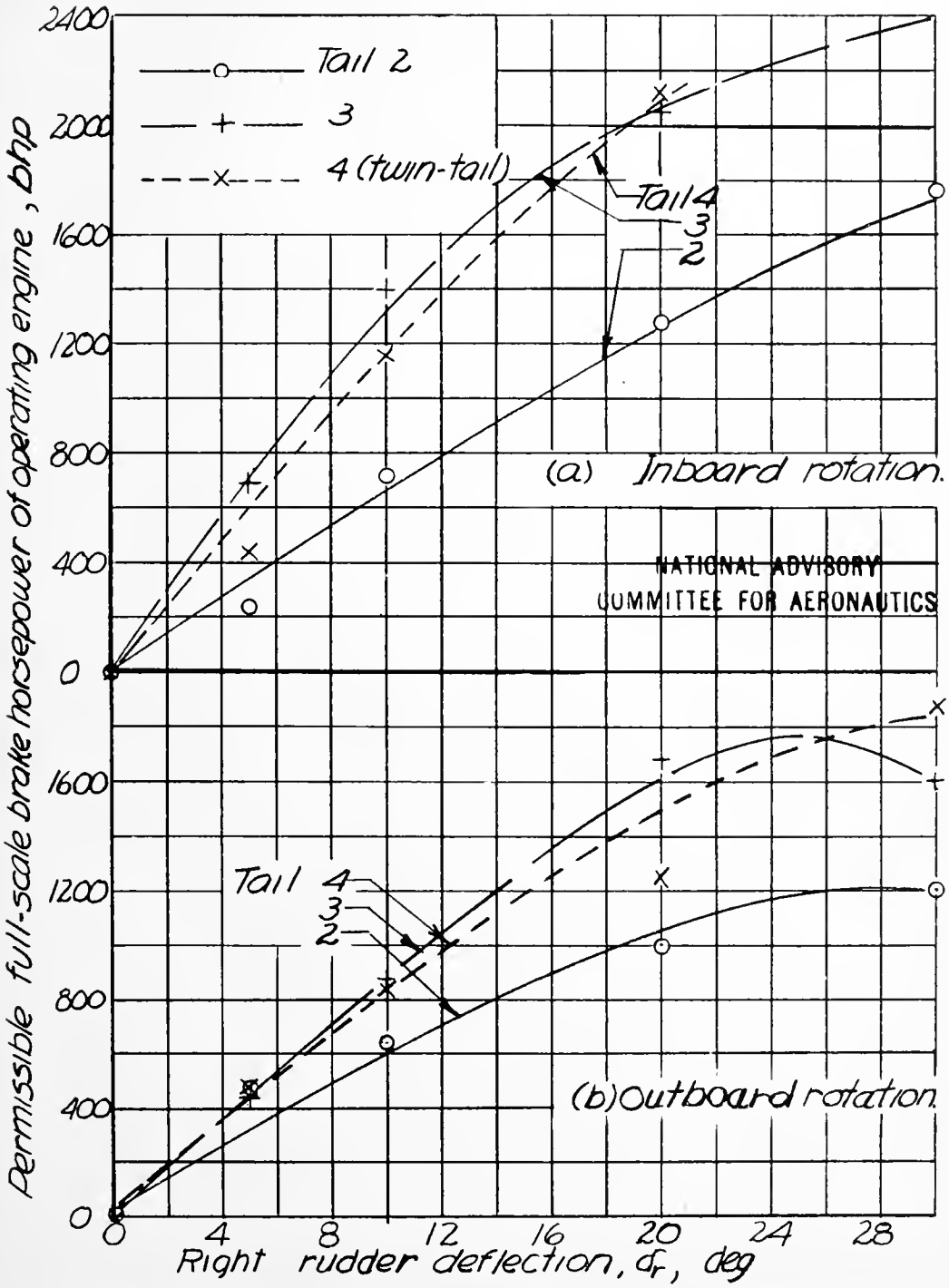

Figure 21.- Comparison of the asymmetric-power characteristics of an airplane equipped with twin and single vertical tails. NACA specifications; $\beta = 0°$.

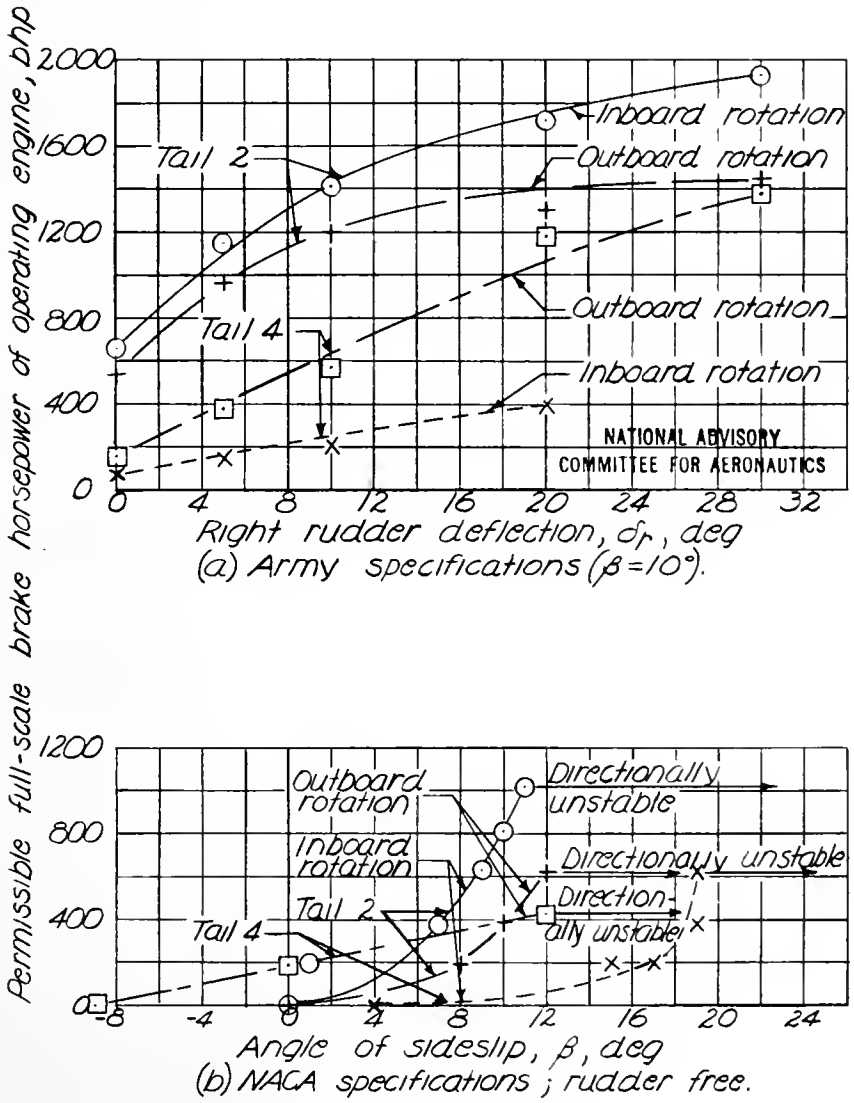

Figure 22.- Comparison of the asymmetric-power characteristics of an airplane equipped with twin and single vertical tails and at various angles of sideslip.

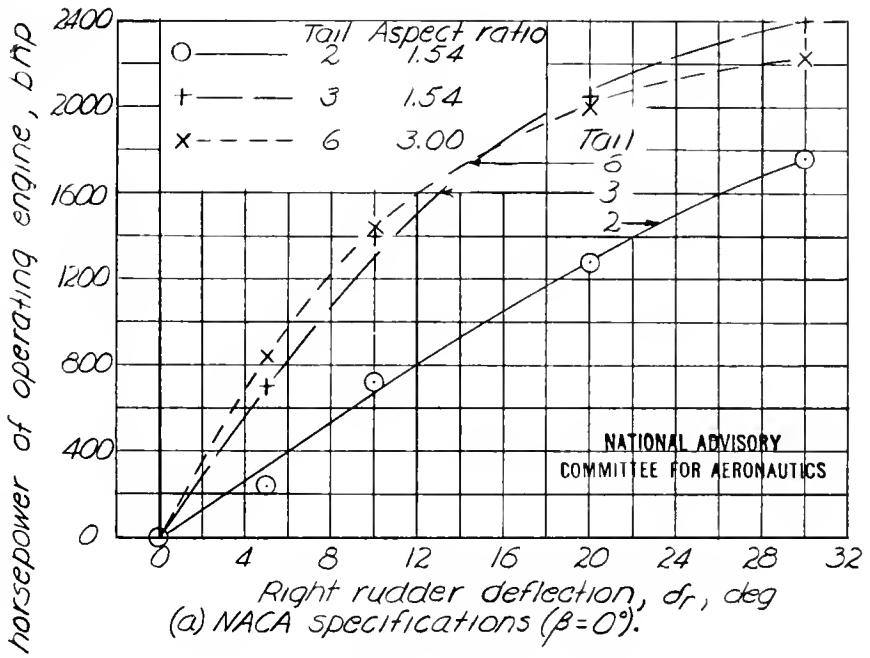

(a) NACA specifications ($\beta = 0°$).

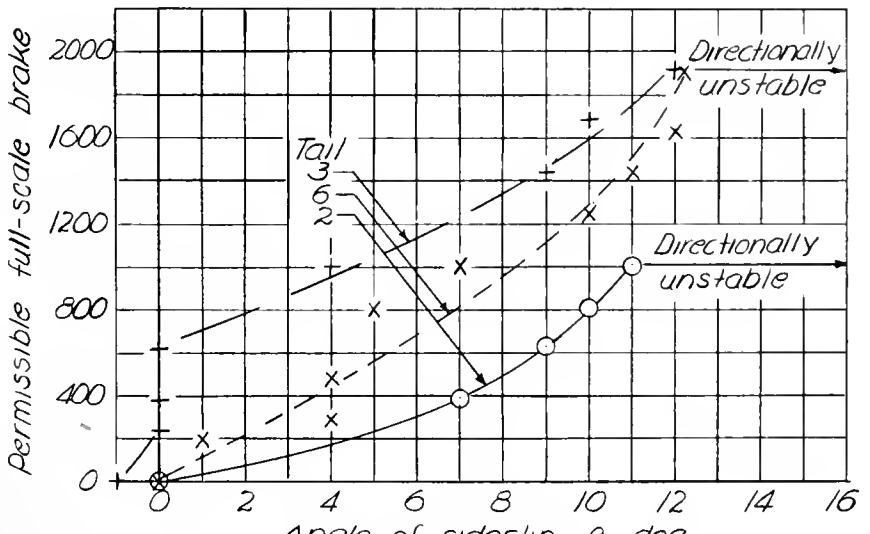

(b) NACA specifications; rudder free.

Figure 23.- Comparison of the asymmetric-power characteristics of an airplane equipped with high- and low-aspect-ratio vertical tails. Inboard rotation.

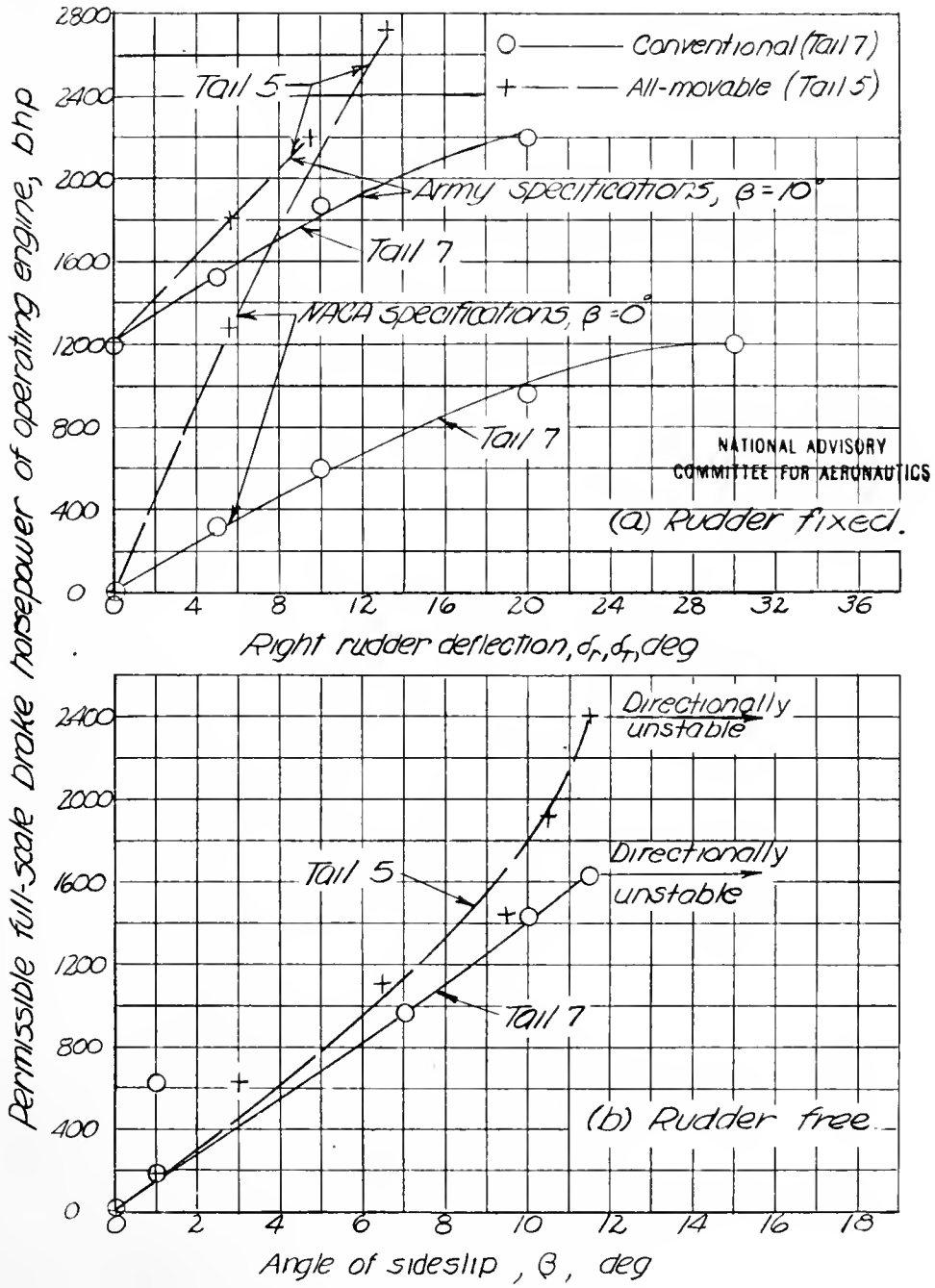

Figure 24.- Comparison of the asymmetric-power characteristics of a twin-engine-airplane model equipped with an all-movable vertical tail with linked tab and with a single conventional tail. Operating propeller turning outboard.

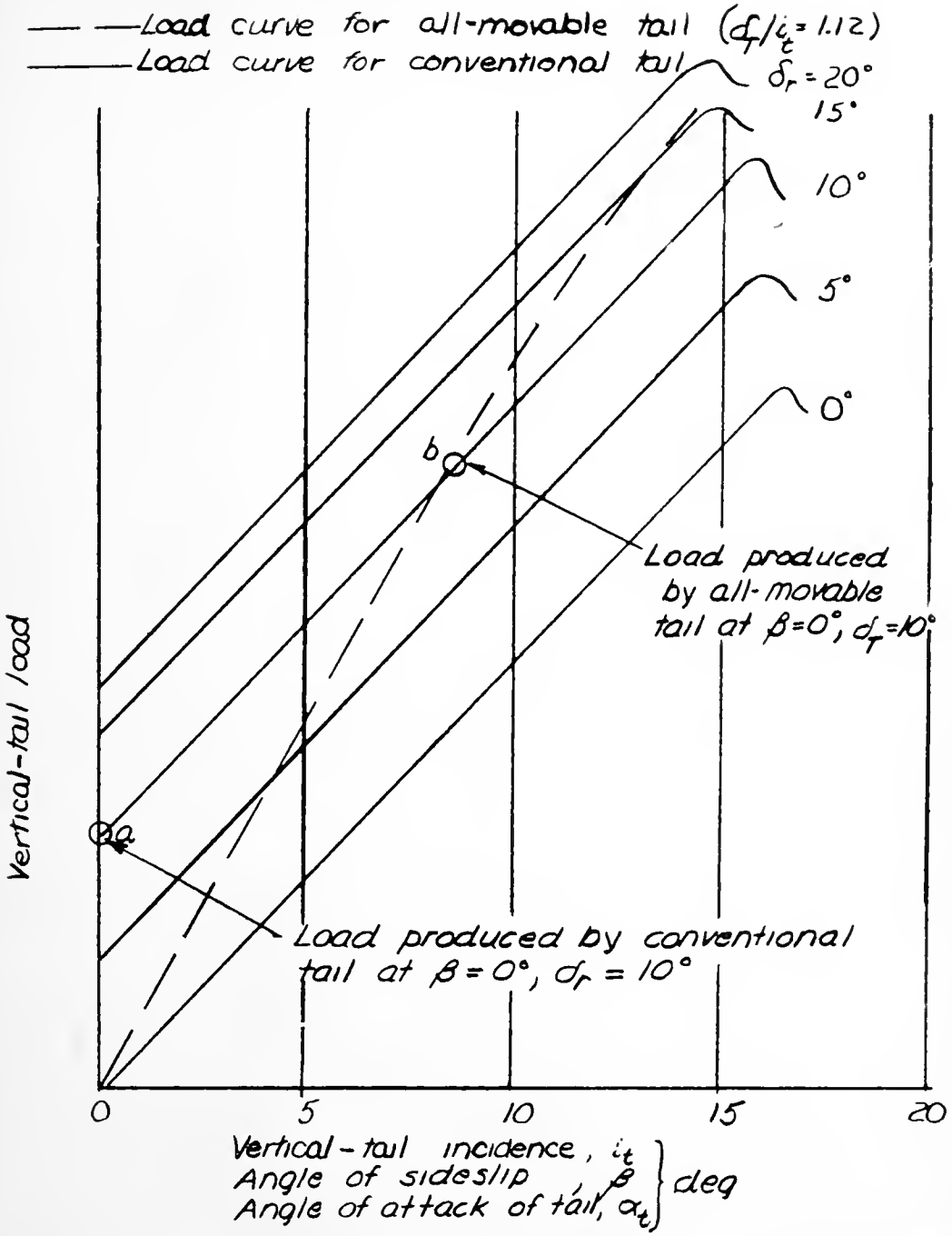

Figure 25.- Typical load curves for the all-movable and conventional types of vertical tail.

NATIONAL ADVISORY
COMMITTEE FOR AERONAUTICS

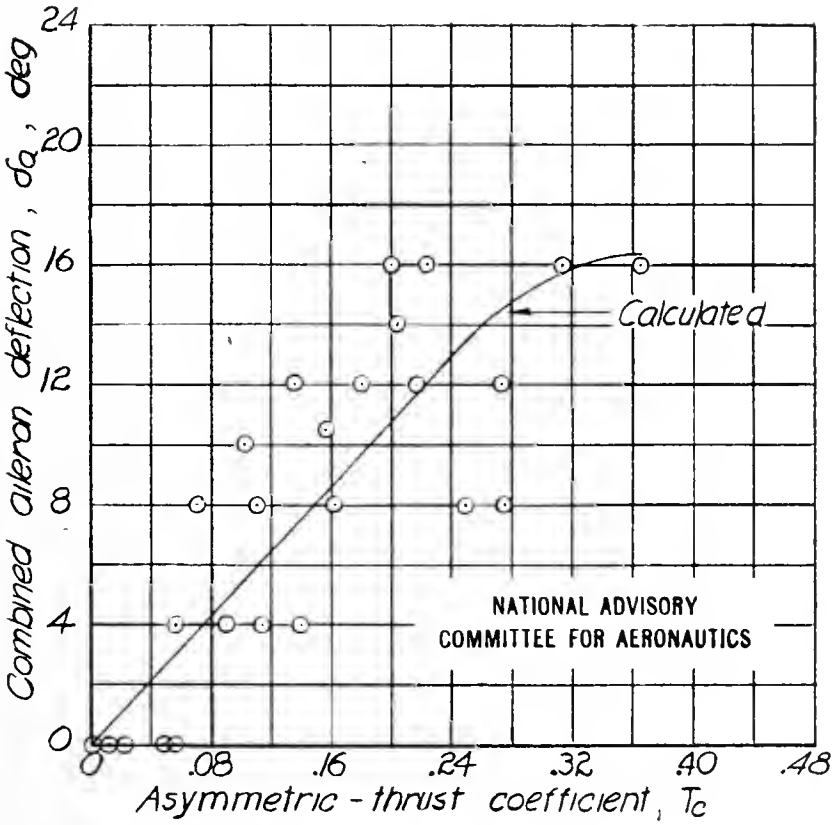

Figure 26.— Aileron deflections required to trim rolling moment created by asymmetric power. $\beta = 0°$; operating propeller rotating outboard.